PHOTOGRAPHIC SCIENCE AND ENGINEERING

Some Aspects of the Mechanism of Development with a Substituted p-Phenylenediamine: The Kinetics of Physical and Chemical Development
R. B. Pontius and Joan S. Thompson 45

Electronmicroscopic Investigations of Photographic Layers • *E. Klein* 52

Effects of Some Organic Compounds on Zeta-Potential of Silver Bromide
Shin Suzuki and Yasushi Oishi 56

Control of Low-Intensity Reciprocity Law Failure with Mercaptooxazoline Development Retarders • *Ernest T. Larson and Harold A. Levine* 59

Wedge Brittleness Test for Photographic Film • *P. Z. Adelstein* 63

The Fundamental Nature of Curl and Shrinkage in Photographic Films • *J. Q. Umberger* 69

A Color Chart for Use in Evaluating Quality of Color Reproduction
Edwin J. Breneman 74

Technicalia Photographica • *Frank Smith* 79

Book Reviews 91

OCTOBER • 1957

Volume 1 • Number 2

Editorial Policy

Photographic Science and Engineering is dedicated to the advancement of the knowledge and application of photography and other directly related sciences. Its pages are open to all who wish to report on new studies dealing with the theory of photosensitive systems, the design of photographic instruments and apparatus useful in the treatment of photographic materials, photographic optics and illuminants, the use of photography for scientific or engineering measurement or recording, and photographic instrumentation and data recording. Only original papers should be submitted except on special invitation.

Manuscripts should be typed double-spaced on white bond paper with $1^1/_4$-inch margins all around. Literature references should be exact, and should include titles of papers and journals, names of authors, numbers of volumes and pages, and year of publication. Book references should include title of volume, names of authors, publisher, number of edition, year of publication, and chapter and pages cited.

Graphs, charts, and other line illustrations should conform to good usage such as given in the American Standards Association Document Y-15, "A Guide for Preparing Technical Illustrations for Publication and Projection." Continuous-tone photographs should be made on 8- by 10-inch glossy paper and should show pertinent image detail sufficiently clearly to permit reduction to fit a 3-inch column in this journal. All illustrations should be numbered in soft blue pencil on the back to correspond with captions typed on a separate page. Tables should also be submitted on separate pages appropriately identified. An abstract should accompany each manuscript.

All papers submitted for publication will be reviewed by members of the Editorial Review Board and if not accepted will be returned to the author, provided a self-addressed envelope and specific instructions are furnished. Published papers become the property of the Society and are protected by appropriate copyrights. Authors receive five copies of issues in which their contributions appear. Additional copies and reprints may be obtained. The Society does not assume responsibility for material in transit, nor guarantee publication of unsolicited material.

PHOTOGRAPHIC SCIENCE AND ENGINEERING

official publication of the
Society of Photographic Scientists and Engineers

OCTOBER 1957
Volume 1, Number 2

EDITORIAL STAFF

Peter Krause, Editor
Jennie H. Allen, *Managing Editor*
Frank Smith, *Feature Editor*
Edward K. Kaprelian, *Feature Editor*
Willard W. Van Allen, *Associate Editor*
Jean St. Thomas, *Foreign Editor*

EDITORIAL REVIEW BOARD

T. H. James, *Chairman*
R. S. Barrows
R. C. Davis
H. E. Edgerton
K. G. Leistner
J. A. Maurer
H. F. Nitka
J. H. Waddell

Photographic Science and Engineering is published four times a year by the Society of Photographic Scientists and Engineers. Publication office at 20th and Northampton Streets, Easton, Pa. Address correspondence to the Society at Box 1609, Main Post Office, Washington, D.C. Subscription to non-members of the Society, $8.00 per year; single copies, $2.00 each. The Society is not responsible for the accuracy of statements made by authors and does not necessarily subscribe to their views. Application for entry as second class matter at the Post Office, Easton, Pa., is pending.

© Copyright 1957 by the Society of Photographic Scientists and Engineers, Inc. Permission to reprint any part of the contents, except in reviews and abstracts, must be obtained in writing from the Editorial Vice President.

PHOTOGRAPHIC SCIENCE AND ENGINEERING
Volume 1, Number 2, October 1957

Some Aspects of the Mechanism of Development with a Substituted *p*-Phenylenediamine: The Kinetics of Physical and Chemical Development

R. B. PONTIUS AND JOAN S. THOMPSON, *Research Laboratories, Eastman Kodak Company, Rochester, N.Y.*

The kinetics of postfixation physical development of Eastman Fine Grain Release Positive Film, Type 5302, with the color developer, 4-amino-3-methyl-N-ethyl-N-(β-methylsulfonamidoethyl)-aniline, have been determined. Evidence is presented for development by a *p*-phenylenediamine developer while adsorbed to silver and a direct comparison is made between the kinetics of chemical and pure physical development by the same developer. Chemical development is at least an order of magnitude faster than physical development in the absence of silver halide solvent. If sufficient silver halide solvent is present, chemical development predominates in the early stages but is rapidly supplemented by physical development.

A practical color developer is a derivative of *p*-phenylenediamine and, in general, is one of the *p*-amino-N,N-dialkylanilines.[1,2] Color development usually refers to the formation of a dye in a photographic emulsion by the simultaneous development of exposed silver halide and condensation of the oxidized developer with an added color-forming molecule or "coupler" to form the dye.[3] Apart from the coupling reaction,[4,5] the mechanism of the reduction of silver halide by the color developer is an important question in photographic theory, and one which has already been studied to some extent by James[6] and Fortmiller.[7] Two questions about the development process which have not been fully resolved are (a) whether or not the reduction of silver halide by *p*-phenylenediamine developers is a catalyzed process initiated at the interface between the latent image and the silver halide, as appears to be the case for developers of the Elon*-hydroquinone type,[8] and (b) whether or not physical development plays an important part in development with substituted *p*-phenylenediamine developers. In the present paper an attempt will be made to give an answer to the second question.

The first act in development is probably the adsorption of the developing agent at the site of the reaction.[9] There is evidence to indicate that the *p*-phenylenediamines do differ fundamentally from Elon and hydroquinone in their mode of adsorption.

James has studied the rate of silver development by several developing agents, both in photographic emulsions and in solution where the silver ion is present as a soluble complex.[8,10–12] In the study of direct chemical development of silver halide by hydroquinone catechol, hydroxylamine, and *p*-phenylenediamine, James found that, in each case, the rate varied as a fractional power (approximately 0.5) of the developer concentration. If adsorption occurs, and follows the Freundlich isotherm, the rate will reveal a fractional-power dependence upon the developer concentration, as was found by James. The kinetic evidence thus derived by direct chemical development allows one to infer that, with both hydroquinone and *p*-phenylenediamine, development occurs after adsorption. Other evidence for adsorption of the various developing agents to silver bromide is provided by the work of James and Vanselow on the adsorption of photographic materials on silver bromide chromatographic columns.[13]

In solution, in the presence of silver ion and colloidal metal catalyst, James found that, with hydroquinone, catechol, and ascorbic acid, the development rate varies as the first power of the developer concentration, implying that the developer *is not* adsorbed to the silver. However, the development rate with *p*-phenylenediamine, hydrazine, and hydroxylamine varies as a fractional power of the developer concentration, which suggests that these agents adsorb to the silver catalyst.[12,14] Perry, Ballard, and Sheppard[15] found by direct measurement that Elon and hydroquinone do not adsorb to silver, at least to an extent greater than ten per cent of the surface coverage.[16] No corresponding direct measurements for the case of the *p*-phenylenediamines have

Communication No. 1907 from the Kodak Research Laboratories. Received 7 June 1957.

* Kodak Elon Developing Agent, trade name of Eastman Kodak Company for N-methyl-*p*-aminophenol sulfate.

been made. Thus, there is evidence that black-and-white and *p*-phenylenediamine developers adsorb to silver halide, and develop while in the adsorbed state. There is indirect evidence that *p*-phenylenediamine also adsorbs to metallic silver and may develop while adsorbed to silver. Additional evidence of a difference in the mode of action of substituted *p*-phenylenediamine developers and black-and-white developers is provided by work on autoxidation by Weissberger and Thomas.[17] They found that, while silver produced very little acceleration of the autoxidation of hydroquinone, catechol, *p*-aminophenol, and glycine, the autoxidation of *p*-phenylenediamine and *p*-dimethylaminoaniline showed a considerable catalysis by silver.

The view that developers of both general kinds, the common black-and-white developers and the *p*-phenylenediamines, give direct development by a catalyzed reaction at the interface between the silver halide and the latent image, and also may produce fog by a slower uncatalyzed reduction, while the developers are adsorbed to the silver halide, has considerable support, although this view cannot be regarded as proved, especially in the case of the *p*-phenylenediamine developers. However, the important question arises whether or not there exists an additional process whereby a *p*-phenylenediamine acts while adsorbed to the silver of the latent image. The experiments described here show that, although a practical *p*-phenylenediamine developer can act while adsorbed to the latent image in a case where there is no possibility of adsorption to silver halide, this pure physical development process is an order of magnitude too slow to account for the normal direct reduction of silver halide by the developer.

Postfixation Physical Development—Method

Development in solution by *p*-phenylenediamine in the presence of colloidal metallic catalyst in the absence of silver halide was used by James[12] to show a dependence of development rate on a fractional power of the developer concentration and thus to infer adsorption of the developing agent to the colloidal metallic catalyst. In the present work, postfixation physical development is used, the silver of the latent image serving to initiate the reduction. The use of an emulsion, in this case Eastman Fine Grain Release Positive Film, Type 5302, makes it possible, not only to show the kinetics of purely physical development, but also to measure the development rate by direct or "chemical" development, without prefixation, and thus to compare directly the relative rates of physical and chemical development.

The physical developer used was one suggested by E. E. Jelley, of these Laboratories. In it the silver-thiosulfate complex is the source of silver ion. The developing agent, 4-amino-3-methyl-N-ethyl-N-(β-methylsulfonamidoethyl)-aniline, was used in a series of concentrations, with and without an added coupler, H-acid (8-amino-1-naphthol-3,6-disulfonic acid). The film samples, 35mm wide, were uniformly exposed

TABLE I

Composition of Physical Developer (When Used with the Soluble Coupler, H-Acid)

Component A	
4-amino-3-methyl-N-ethyl-N-(β-methylsulfonamido-ethyl)-aniline-sesqui-sulfate	2.25 g
Sodium carbonate, monohydrate	30.00 g
H-acid	1.67 g
Deaerated distilled water	800.00 ml
Component B	
Sodium chloride	4.4 g
Silver nitrate	4.4 g
Crystalline sodium thiosulfate	25.0 g
Deaerated distilled water	100.0 ml

in a sensitometer at a level of 1.26×10^4 meter-candle-seconds. Before development, the samples were fixed for 4 minutes in an alkaline fixing bath, as described by James, Vanselow, and Quirk.[18] After washing for one-half hour, the strips were developed for periods of 5 to 80 minutes. As all solutions were deaerated before use and processing was carried out with nitrogen agitation, the use of sulfite was unnecessary. After processing, the amount of silver developed in the strips was determined by the Analytical Chemistry Department of these Laboratories. The composition of the developer solution is shown in Table I.

In the preparation of Component B of the developer, the sodium chloride and silver nitrate were dissolved separately; the silver chloride was precipitated and allowed to settle in the dark. The supernatant liquid was then decanted and the precipitate dissolved in the 100-ml solution of sodium thiosulfate. Finally, the silver-thiosulfate complex solution was added to Component A and a dilute solution of sodium hydroxide added to adjust the final pH to 11.7 and volume to 1000 ml. The developer was freshly prepared each time and discarded after use.

Postfixation Physical Development—Results

The effect of developer concentration upon development rate is shown in Fig. 1, where the silver analyses are plotted against development time for a developer containing no soluble coupler (H-acid). These data indicate that the developed silver increases with the square of the development time, at least over most of the development interval. This fact may be shown by plotting the silver analyses against t^2 (Fig. 2). This behavior would be expected if the rate of reduction of silver ion to metallic silver is proportional to the square root of the mass of silver already produced,

$$\frac{dy}{dt} = k_1 y^{1/2}, \qquad (1)$$

where y is the mass (or concentration) of silver present at time t, and k_1 is the specific rate constant. Integration of Equation (1) leads to,

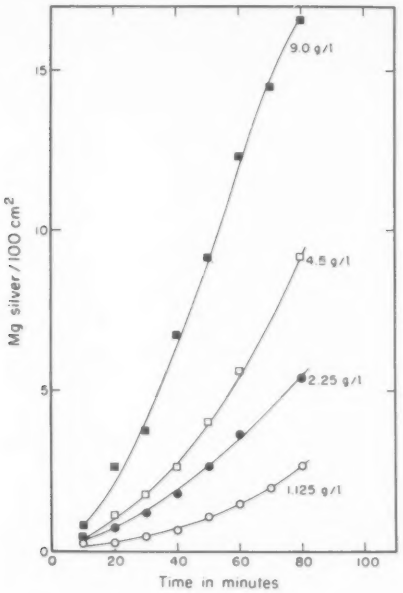

Fig. 1. Rate of postfixation physical development with 4-amino-3-methyl-N-ethyl-N-(β-methylsulfonamidoethyl)-aniline and silver-thiosulfate complex. Variation in developer concentration.

$$y = \frac{1}{4} k_1^2 t^2, \tag{2}$$

provided it is assumed that the amount of silver initially present as latent image at time zero is negligibly small in comparison with the silver developed upon the latent-image nuclei.

A plot of y as a function of t^2 should give straight lines with slope $k_1^2/4$. The specific rate constants can, therefore, be obtained from the slopes of the straight-line portions of the curves (Fig. 2). The data are shown in Table II.

TABLE II

Specific Rate Constants for the Reduction of Silver Ion in Postfixation Physical Development without Soluble Coupler

Concentration (C) of Developer, g/l	$\log_{10} C$	Specific Rate Constant (k_1)	$\log_{10} k_1$
1.125	0.052	3.98×10^{-2}	−1.400
2.25	0.352	6.10×10^{-2}	−1.214
4.50	0.654	7.46×10^{-2}	−1.127
9.0	0.954	11.4×10^{-2}	−0.943

The Freundlich isotherm, which describes many cases of adsorption, is expressed by

$$C_a = KC^{\alpha}, \tag{3}$$

where C_a is the concentration in the adsorbed phase, C is the concentration in solution, which may be taken

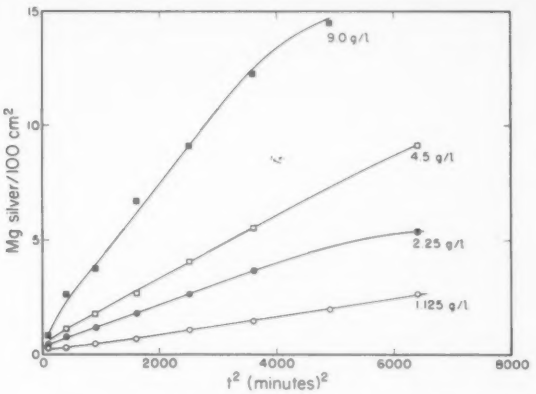

Fig. 2. Postfixation physical development with 4-amino-3-methyl-N-ethyl-N-(β-methylsulfonamidoethyl)-aniline and silver-thiosulfate complex. Analyses of silver developed as a function of the square of the development time.

as the initial concentration, K is a constant, and α is a fraction. If the specific rate constant, k_1, is proportional to the developer concentration in the adsorbed phase, one can write

$$k_1 = K'C^{\alpha}, \tag{4}$$

and

$$\log k_1 = \log K' + \alpha \log C. \tag{5}$$

Thus, a plot of $\log k_1$ on the y-axis against $\log_{10} C$ on the x-axis should give a straight line with slope α.

$\log_{10} k_1$ is plotted against $\log_{10} C$ in Fig. 3. The slope of the line (Fig. 3) is 0.51, so one finds that the specific rate constant k_1 is given by

$$k_1 = K'C^{0.51}. \tag{6}$$

The fractional exponent, 0.51, in Equation (6) suggests that the developer, 4-amino-3-methyl-N-ethyl-N-(β-methylsulfonamidoethyl)-aniline, adsorbs to the silver and reduces silver ion while the developer is in the adsorbed state, in agreement with earlier results obtained by James[12] in the case of p-phenylenediamine and colloidal silver and gold nuclei.

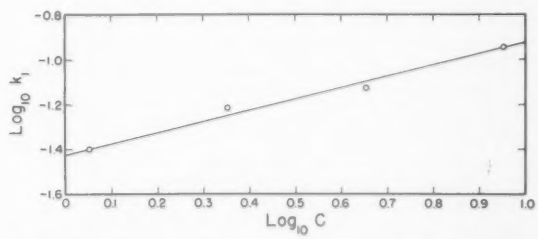

Fig. 3. Determination of the exponent in the Freundlich adsorption isotherm from results of postfixation physical development with 4-amino-3-methyl-N-ethyl-N-(β-methylsulfonamidoethyl)-aniline. Logarithm of the specific rate constant, k_1, against the logarithm of the developer concentration, C.

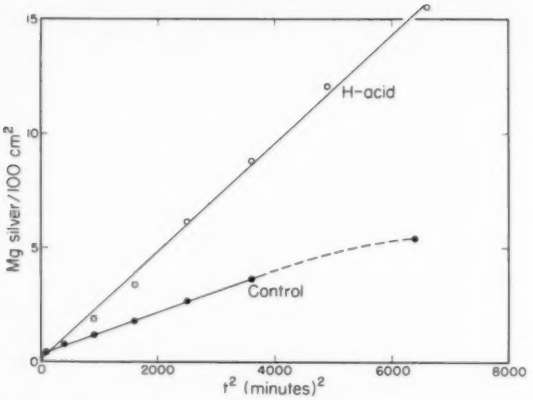

Fig. 4. Effect of soluble coupler (H-acid) on postfixation physical development with 4-amino-3-methyl-N-ethyl-N-(β-methylsulfonamidoethyl)-aniline and silver-thiosulfate complex. Analyses of silver developed as a function of the square of the development time.

Effect of Soluble Coupler on Physical Development

It is known[6] that direct development of silver halide by a *p*-phenylenediamine is accelerated in the presence of a coupler which reacts with the oxidation product of the developer. Such a coupler also accelerates physical development by a *p*-phenylenediamine; this was shown by repeating the experiment with a developer concentration of 2.25 g/l with the addition of 1.7 g/l of H-acid. A comparison of the rates of development, with and without coupler, are shown in Fig. 4, where, as before, the silver analyses are plotted against the square of the time. The effect of the coupler was to increase the specific rate constant from 0.061 to 0.097 $(mg/100\ cm^2)^{1/2}\ min^{-1}$, a 59 per cent increase in development rate.

Comparison of Chemical and Physical Development Rates

Pure physical development by the *p*-phenylenediamine developer proceeds at an initially slow rate, and increases as the amount of silver produced increases. Direct or "chemical" development proceeds by a different mechanism and, in the case of most of the substituted *p*-phenylenediamines, has its greatest rate in the early stages of development. The problem of the relative rates of physical and chemical development has been attacked by James and Vanselow,[19] who have compared the two rates as a function of silver halide solvent. The rates of chemical and physical development can also be compared by measuring the specific rate constant for chemical development in the same emulsion previously used for postfixation physical development, without the prefixation, and without added silver ion or silver halide solvent in the developer.

The chemical developer used was formulated as a good surface developer, showing very little evidence of solvent action. The soluble coupler (H-acid) was used. The physical and chemical developers were closely similar with respect to pH and developer concentration and hence may be considered approximately equivalent. Although the physical developer at the high developer concentration did not contain coupler, the increase in rate of physical development caused by added coupler was already determined so that the approximate increase in rate which would have been obtained by added coupler could be taken into account. A comparison of the two developers used is shown in Table III.

Typical rate curves for chemical development are shown in Fig. 5, the upper for a shoulder exposure (the logarithm of the exposure in meter-candle-seconds was equal to 1.90), the middle for a toe exposure (the logarithm of the exposure in meter-candle-seconds was equal to 0.50), and the lowest curve for fog production in an unexposed area. Apparently, fog is formed by a mechanism different from that of image development.

The rate curve for chemical development in the shoulder of the H and D curve (upper curve, Fig. 5) is more nearly characteristic of what is generally called "chemical development," and evidently is due to quite a different mechanism from that operating in

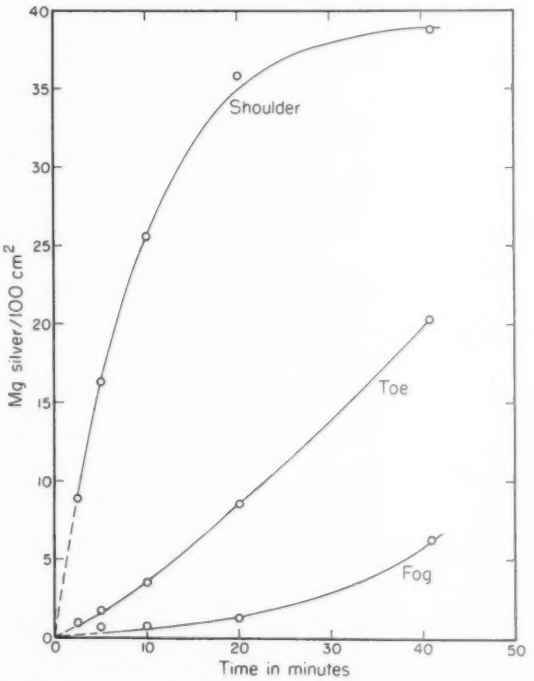

Fig. 5. Direct chemical development of Eastman Fine Grain Release Positive Film, Type 5302, with 4-amino-3-methyl-N-ethyl-N-(β-methylsulfonamidoethyl)-aniline at pH 12: Top curve—development rate for exposure on the shoulder of the H and D curve. Middle curve—development rate for exposure on the toe of the H and D curve. Bottom curve—development rate for fog formation in unexposed emulsion.

TABLE III
Composition of Physical and Chemical Developers

Component	Concn. of Components in Physical Developer	Concn. of Components in Chemical Developer
Developing agent	9.0 g/l	8.0 g/l
Sodium sulfite	—	2.0 g/l
Potassium bromide	—	2.0 g/l
H-Acid	—	2.0 g/l
Added silver ion	2.6 g/l	—
Temperature	75F	75F
pH	11.7	12.0

physical development. Following James,[16] the rate of chemical development can be represented by the equation,

$$\frac{dy}{dt} = k_2(y_0 - y), \tag{7}$$

where y is the amount of silver reduced (here expressed in mg/100 cm^2), y_0 is the maximum amount of silver available as silver halide, and k_2 is the specific rate constant. Integration of Equation (7) leads to the expression,

$$\log_e(y_0 - y) = -k_2 t + \log_e y_1. \tag{8}$$

The data for the upper curve of Fig. 5 have been used to plot, in Fig. 6, the values of $\log_{10}(y_0 - y)$ against t. The specific rate constant, k_2, is the slope of the straight line (Fig. 6) multiplied by 2.303. The value of k_2 is 0.19 min^{-1}. Had soluble coupler been used in the physical developer, the comparable rate constant for physical development, k_1, would have been approximately 0.18 (mg/100 cm^2)$^{1/2}$ min^{-1}. However, because the mechanism is different in the two cases, the rate constants have different dimensions and cannot be compared directly. Furthermore, since the actual rate of chemical development decreases with time while that of physical development increases, any comparison at equal times must be arbitrary. A suitable comparison of the development rates would appear to be one in which both processes start from equivalent latent images and have equal chances.

The present data on physical development rate have been derived from postfixation development. Since there is a possibility that some of the latent image may have been destroyed in the fixing process, it would appear that the two rates should be compared only under the condition that measurable quantities of silver have been produced in each type of development, where the rates are not limited by any process of nucleation. A fair comparison would appear to be at a stage where 1 mg of silver per 100 cm^2 is present in both cases.* The rate of reduction $(dy/dt)_1$ for physical development at the stage where 1 mg of silver per 100 cm^2 has been produced can be calculated from Equation (1) to be 0.18 (mg of silver per 100 cm^2) min^{-1}. The rate of reduction $(dy/dt)_2$ by chemical development at the same stage can be calculated from Equation (7). The maximum silver available, y_0, is approximately 39 mg/100 cm^2, and, therefore, $(dy/dt)_2$ becomes 7.2 (mg of silver per 100 cm^2) min^{-1}. At this stage, the ratio of the rate of chemical development to rate of physical development is 7.2/0.18 or a factor of 40. If the relative rates are calculated at a further stage where 10 mg of silver per 100 cm^2 has been produced, the factor is reduced to approximately 10. The average ratio of chemical development rate to physical development rate in this interval is approximately 25.

* The silver produced in postfixation physical development consists of very thin platelets which probably have a smaller ratio of surface to mass than do the fine silver filaments produced in typical chemical development.

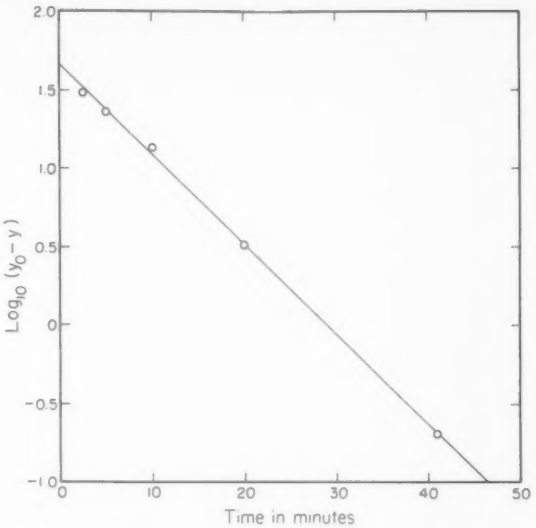

Fig. 6. Determination of rate constant for direct chemical development of Eastman Fine Grain Release Positive Film, Type 5302, with 4-amino-3-methyl-N-ethyl-N-(β-methylsulfonamidoethyl)-aniline at pH 12. Logarithm of the available silver halide per unit area against the development time in minutes. Emulsion given shoulder exposure.

Discussion

The experiments which have been described may be taken to indicate that 4-amino-3-methyl-N-ethyl-N-(β-methylsulfonamidoethyl)-aniline (color-developing agent) is able to act as a developing agent while adsorbed to silver, but that the pure physical development process is an order of magnitude too slow to account for the direct development of silver halide. It may, however, be worth while to inquire why the rate of "physical" reduction should be proportional to the concentration of silver to the one-half power. The picture of physical development postulated is one in which developer adsorbs to the surface of the silver and reduces silver ion or silver complex which diffuses up to the surface. *A priori*, the rate of reduction would be expected to be proportional to the amount of surface available and to

the concentration of silver ion. Since the amounts of silver complex are large, the concentration of this component may be considered effectively constant, and hence the rate of development should be proportional to the surface. The surface is proportional to the two-thirds power of the mass, and the rate equation would be

$$\frac{dy}{dt} = k' y^{2/3}, \tag{9}$$

which leads to a dependence of silver concentration (y) upon the cube of the time, a dependence which is clearly not shown over any appreciable range. If the exponent in the rate equation (1) is 1/2 instead of 2/3, the growth of silver will be less than directly proportional to the surface. This behavior may be due to several possible causes: (1) some of the surface is not available for reduction; (2) some other factor may be rate-limiting, for example, the rate of adsorption of developer or the rate of diffusion of silver ion; or (3) the surface may be poisoned by a slowly desorbed oxidation product. It has been shown in the preceding section that H-acid, which couples with the oxidation product, is an accelerator for the reduction reaction. The acceleration of development by the coupler is commonly regarded as the result of removal of the developer oxidation product, the quinonediimine, from the site of the reaction. The coupling reaction takes place in the aqueous phase while the kinetic data indicate that reduction takes place in the adsorbed phase. An accumulation of quinonediimine in the aqueous phase would hinder desorption of the oxidation product, so coupling of H-acid with the quinonediimine could aid desorption by reducing the local concentration of oxidized developer. However, it will be noted that the rate kinetics still follow very well the one-half-power dependence upon silver concentration (Fig. 4) even when H-acid is present, so that coupling evidently does not increase the amount of surface available. In order to explain the acceleration caused by the coupler, it may be suggested that a mechanism discussed by Vittum and Weissberger[3] may be important. In this mechanism, the quinonediimine is not regarded as the primary oxidation product, but instead the semiquinone ion is first formed, undergoes electrolytic dissociation to the neutral semiquinone, and forms the quinonediimine and the developer by disproportionation. Coupling away of the quinonediimine would displace the reaction away from the semiquinone and would thus increase the local developer concentration.

Simultaneous Physical and Chemical Development

Since the rate of physical development increases with time, while that of chemical development decreases, the contribution of physical development to the over-all rate will increase with time. If physical and chemical development occur simultaneously, as in a developer containing silver halide solvent, the rate of physical development will be very much accelerated, since silver produced rapidly by chemical development will supply surface for physical development.

The rate of physical development must now depend upon both y_1, the physically developed silver, and y_2, the chemically developed silver, and also on the first power of the local silver-ion concentration, $[Ag^+]$,

$$\frac{dy_1}{dt} = k_1[Ag^+]\,(y_1 + y_2)^{1/3}. \tag{10}$$

The rate of chemical development is now reduced by the loss of silver halide by solvent action. The silver formed by physical development cannot exceed that lost from the silver halide by solvent action. If the rate of solution, and, therefore, the supply of silver ion is rate-limiting, then all the ion supplied is physically developed, and the rate of physical development may be less than that calculated for an excess of silver ion. Only cases where considerable solvent action is present will therefore be considered in this discussion. In order to show how the ratio of chemical to physical development may change during the course of development, the hypothetical case may be discussed, in which the amount of silver physically developed, y_1, equals that lost from the silver halide, and yet is not rate-limiting so that Equation (10) will be applicable. Products of development, such as bromide and iodide, which were absent in pure physical development, may, of course, modify the rate of solution and therefore the physical development rate when silver halide is present. It is to be understood that the purpose of this calculation is merely to demonstrate how chemical and physical development may supplement each other, and the results are not intended to be quantitative. One can write, for the rate of chemical development,

$$\frac{dy_2}{dt} = k_2\,(y_0 - y_1 - y_2). \tag{11}$$

It is readily possible to compare the rates as a function of the total mass of silver produced. The ratio of the two rates is

$$\frac{\frac{dy_2}{dt}}{\frac{dy_1}{dt}} = \frac{k_2}{k_1(Ag^+)} \cdot \frac{y_0 - (y_1 + y_2)}{(y_1 + y_2)^{1/3}}. \tag{12}$$

The analytical methods cannot distinguish between y_1 and y_2, so one can replace $y_1 + y_2$ simply by y, the total silver. The rate constant, k_2, is known for the case of chemical development, and k_1 is known for a particular concentration of silver complex, 2.5×10^{-2} mole per liter. Ordinary solvent action cannot supply this large a concentration of silver ion. Consider a smaller concentration, say, one-half the amount used in the experiment to determine k_1, that is, replace $k_1(Ag^+)$ arbitrarily by $k_1/2$. The ratio of the rate of chemical development to rate of physical development is then given by

$$\frac{2k_2(y_0 - y)}{k_1 y^{1/3}}. \tag{13}$$

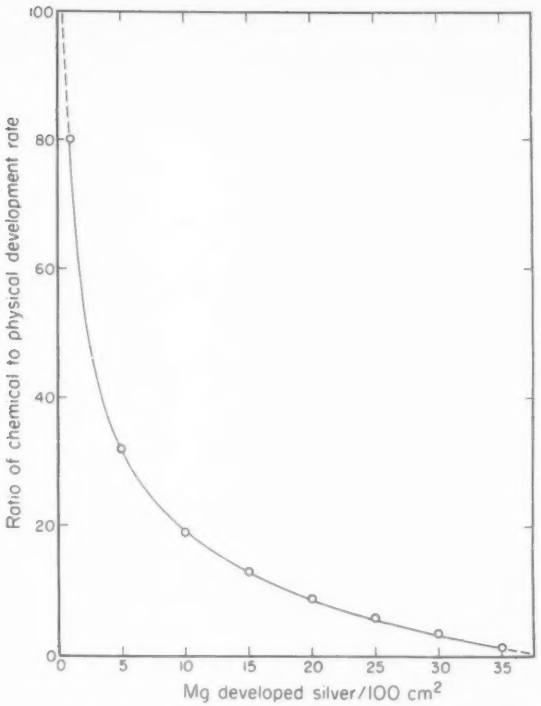

Fig. 7. Comparison of the rate of chemical development to the rate of physical development by a substituted *p*-phenylenediamine developer in a hypothetical case where silver halide solvent is present and both types of development occur simultaneously. On the x-axis the amount of silver developed is an increasing function of the development time.

The ratios of rates of chemical to physical development calculated from Equation (13) are plotted in Fig. 7 as a function of total silver. The curve shows that chemical development is the dominating mechanism early in development but if silver halide solvent is present, physical development begins to contribute to the development very rapidly.

Summary

1. Pure physical development with 4-amino-3-methyl-N-ethyl-N-(β-methylsulfonamidoethyl)-aniline takes place, with the developer acting while adsorbed to the metallic silver.
2. The rate of physical development is approximately proportional to the square root of the amount of silver produced; the rate of development increases with time.
3. Soluble coupler accelerates physical as well as direct development by the *p*-phenylenediamine developer. The acceleration by the coupling of the oxidized developer may be the result of a displacement of the disproportionation equilibrium whereby totally reduced developer and fully oxidized developer are formed from the semiquinone.
4. Pure physical development is very much slower than pure chemical development when both processes are initiated by the latent image.
5. The silver-catalyzed reduction of silver halide by the *p*-phenylenediamine ("direct" or "chemical" development) is a process distinct from the reduction of silver ion from solution. Physical development may occur simultaneously with chemical development, but, unless silver halide solvent or added silver ion is present, chemical development is the principal mode of action.
6. Chemical development with 4-amino-3-methyl-N-ethyl-(β-methylsulfonamidoethyl)-aniline consists of one mechanism for development of heavily exposed areas, and a different mechanism for the nucleation process or fog formation. Characteristic chemical development of fully exposed grains follows an exponential law, the rate decreasing with time.
7. When silver halide solvent is present, the silver rapidly produced by chemical development supplies a large surface for physical development so that a long induction period for the latter process is avoided. The ratio of chemical to physical development decreases very rapidly with time.
8. It is possible to have cases of pure physical development, but it is doubtful if there are ever any cases of completely pure chemical development, particularly in the later stages.

Bibliography

1. Bent, R. L., Dessloch, J. C., Duennebier, F. C., Fassett, D. W., Glass, D. B., James, T. H., Julian, D. B., Ruby, W. R., Snell, J. M., Sterner, J. H., Thirtle, J. R., Vittum, P. W., and Weissberger, A., *J. Am. Chem. Soc.*, Vol. 78, p. 3100 (1951).
2. Thirtle, J. R., *Phot. Sci. and Technique*, (II) Vol. 3, p. 66 (1956).
3. Vittum, P. W., and Weissberger, A., *J. Phot. Sci.*, Vol. 2, p. 81 (1954).
4. Tong, L. K. J., *J. Phys. Chem.*, Vol. 58, p. 1090 (1954).
5. Tong, L. K. J., and Glesmann, M. C., *J. Am. Chem. Soc.*, Vol. 78, p. 5827 (1956).
6. James, T. H., *Phot. Sci. and Technique*, Vol. 16B, p. 83 (1950); ———, *Phot. Sci. and Technique*, Vol. 17B, p. 27 (1951).
7. Fortmiller, L. J., and James, T. H., *Phot. Sci. and Technique*, Vol. 17B, p. 102, (1951).
8. James, T. H., *J. Chem. Education*, Vol. 23, p. 595 (1946); ———, *J. Chem. Phys.*, Vol. 11, p. 338 (1943); ———, *J. Chem. Phys.*, Vol. 14, p. 536 (1946).
9. Sheppard, S. E., and Meyer, G., *J. Am. Chem. Soc.*, Vol. 42, p. 689 (1920).
10. James, T. H., *J. Phys. Chem.*, Vol. 44, p. 42 (1940); ———, *J. Phys. Chem.*, Vol. 47, p. 597 (1943); ———, *J. Am. Chem. Soc.*, Vol. 61, p. 2379 (1939).
11. Levenson, G. I. P., and James, T. H., *J. Phot. Sci.*, Vol. 2, pp. 169–174 (particularly page 172) (1954).
12. James, T. H., *J. Phys. Chem.*, Vol. 45, p. 223 (1941).
13. James, T. H., and Vanselow, W., *J. Am. Chem. Soc.*, Vol. 74, p. 2374 (1952).
14. James, T. H., *J. Am. Chem. Soc.*, Vol. 61, p. 648 (1939).
15. Perry, E. S., Ballard, A., and Sheppard, S. E., *J. Am. Chem. Soc.*, Vol. 63, p. 2357 (1941).
16. James, T. H., *Advances in Catalysis*, Vol. 2, p. 114. Academic Press Inc., New York (1950).
17. Weissberger, A., and Thomas, Jr., D. S., *J. Am. Chem. Soc.*, Vol. 64, p. 1561 (1942).
18. James, T. H., Vanselow, W., and Quirk, R. F., *PSA Jour.*, Vol. 14, p. 349 (1948).
19. James, T. H., and Vanselow, W., *Phot. Eng.*, Vol. 7, p. 90 (1956).

PHOTOGRAPHIC SCIENCE AND ENGINEERING
Volume 1, Number 2, October 1957

Electronmicroscopic Investigations of Photographic Layers

E. KLEIN, *Research Laboratories, Agfa Aktiengesellschaft fuer Photofabrikation, Leverkusen, Germany*

Direct examination of silver and silver halide crystals under the electron microscope is hampered by the deleterious effects of the radiation on the crystal structure. A technique developed by D. E. Bradley, in which the object to be examined is first covered with a thin carbon skin and is then dissolved to leave the skin replica for examination, was adopted to overcome the shortcomings of the direct method. The technique used for the preparation of specimens is described briefly, the results of the investigations of the macro- and micro-structure of silver halide and developed silver grains are discussed, and sample electronmicrographs shown.

The primary components of a photographic emulsion layer are microcrystals of silver halide which are transformed into small silver aggregates during development. The structure of these particles cannot be discerned under a light microscope and it is necessary to utilize the electron microscope for evaluation of structural details.[1] Direct examination of silver halide and silver crystals under the electron microscope, however, involves the great risk that exposure to the electron beam will alter the crystal structure.[2] For example, the silver halide crystals may be dissociated into silver and free halogen as in photolysis. Moreover, the mobility of the lattice components of silver halide as well as of silver crystals is greatly enhanced under strong electron bombardment, and melt-like phenomena as well as partial evaporation occur; these are favored by an increase in specimen temperature following electron absorption and by the high vacuum in the electron microscope.

Also, the electrons are scattered appreciably by the crystals. Therefore, surface characteristics and fine structural details of the crystals cannot be resolved in a normal specimen since common layer thicknesses are too great to permit non-scattered passage of any electrons. As a result of this scatter the object is reproduced with a uniform density and object-contrast is obscured. All of these difficulties in the direct method of electronmicrography can be avoided by means of a high-resolution replica system.

Bradley[3] described some time ago a new replica method for preparing specimens for electronmicroscopic examination. In this method, the object is exposed to carbon vapor under high vacuum and is covered by a carbon skin. The carbon skin is then reinforced by a plastic layer and the specimen separated from its glass carrier. Next, the object itself is dissolved with the aid of a suitable solvent and then the plastic layer is dissolved, leaving the carbon skin replica which is placed on a conventional carrier for insertion into the electron microscope.

In the present work all carbon evaporation was carried out with a rotating object carrier. This entailed loss of the shadowing effect but yielded uniform coverage of the objects on all sides and made it possible to keep the carbon skin very thin. Skin layers down to 70 Angstrom are sufficiently tough to withstand extensive solvent and water treatments. The silver halide crystals were dissolved by means of a thiosulfate solution, the silver grains with a solution of bichromate. It is well known that carbon skins are very resistant to electron irradiation and that electron scatter is small owing to the thinness of the skin and the low atomic weight of carbon. How-

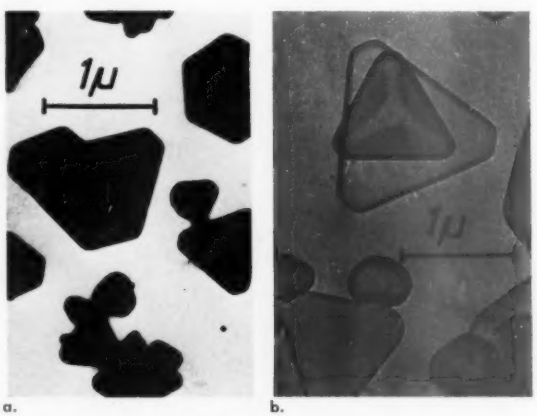

a. b.

Fig. 1. Electronmicrographs of silver bromide crystals of a photographic emulsion: a, direct exposure; b, image of carbon replica.

Read by A. P. Germer, Agfa, Inc., New York, N. Y., at the Annual Conference, Asbury Park, N.J., 12 September 1957. Received 25 August 1957.

ever, electron scatter is sufficiently great to give satisfactory differentiation in the image of thickness variations along the electron paths.

Given below are a few examples of the new information about silver halide crystals and developed silver aggregates, obtained by the carbon-replica technique.

1. *The structure of silver halide microcrystals.* Silver bromide and silver chloride crystallize in a cubic lattice array. The exact form which their microcrystals may take can be explained if individual crystal planes are assumed to be retarded in growth in a certain pattern. In a photographic emulsion the crystal formation occurs during emulsion making and the ultimate shape of the grains is determined by the concentration of excess ions, the concentration of silver halide solvents that promote the formation of complexes and the characteristics of the protective colloid.[4]

The boundary planes of silver bromide crystals usually are 111-planes (octahedron), those of silver chloride 100-planes (cube).

The grains of a photographic emulsion must be freed of all surrounding gelatin prior to examination under the electron microscope and this inevitably leads to some crystal clumping. This is readily seen in Fig. 1, which shows the same crystals of silver bromide photographed directly (Fig. 1a) and by means of the carbon-replica technique (Fig. 1b). The presence of flat, triangular, and three-sided pyramidal type microcrystals is very apparent in the replica reproduction. It was possible to measure exact crystal angles by means of stereo-photographs of this type and to establish without difficulty the development of the pyramidal forms from the basic octahedron configuration.

The gain in information secured by the replica technique is demonstrated further in the comparison images of a pure silver iodide emulsion (Fig. 2). The image obtained through direct exposure in the electron microscope is reproduced in Fig. 2a, and a stereo pair obtained by the replica technique in Figs. 2b and 2c. Crystallographic identification of the six-sided pyramids that can be seen is fairly simple.

2. *Structural details of silver halide crystals.* It is customary to investigate the fine structure of crystals

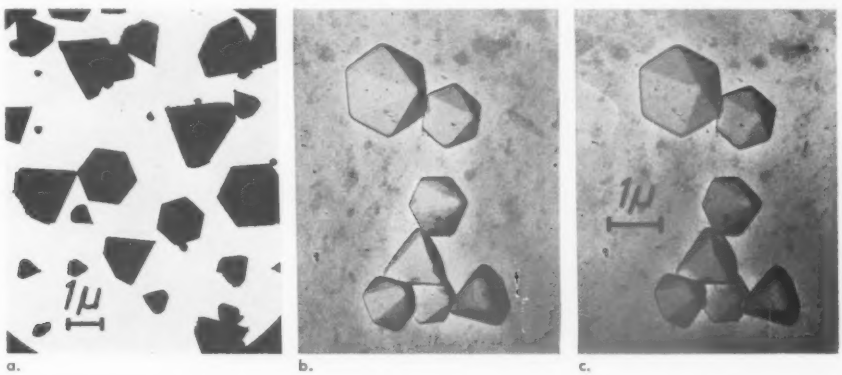

Fig. 2. Electronmicrographs of silver iodide crystals: a, direct exposure; b and c, stereo pair of carbon replica.

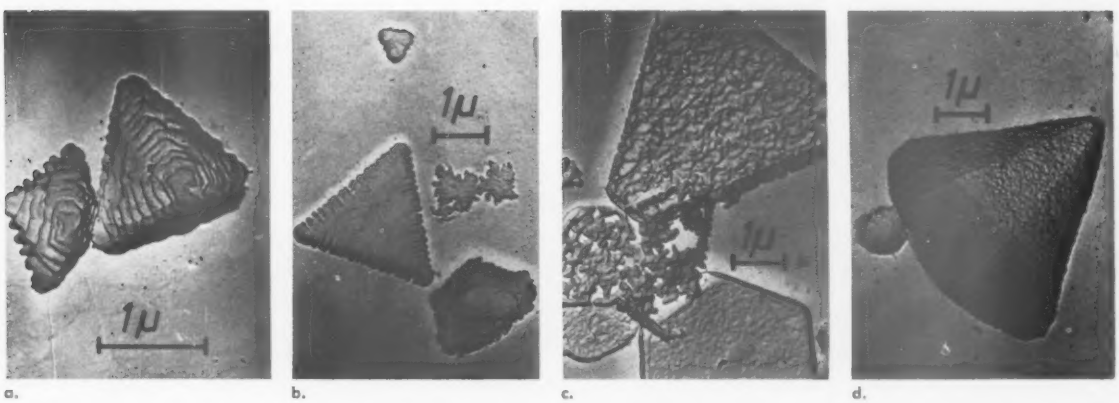

Fig. 3. Electronmicrographs of carbon skins of silver halide crystals etched with sulfite and thiosulfate solutions: a, pyramidal silver bromide crystals (sulfite etch); b, flat triangular silver bromide crystals (sulfite etch); c, flat hexagonal silver bromide crystals (thiosulfate etch); d, silver iodide crystal—six-sided pyramid (sulfite etch).

4.

5.

Figs. 4 and 5. Electronmicrographs of carbon skins of partially developed silver bromide crystals (notice etch-depressions).

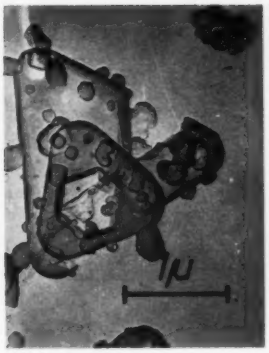

a.

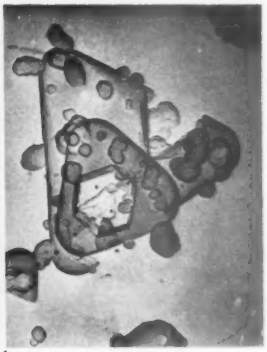

b.

Fig. 6. a and b, Stereo pair of electronmicrographs of carbon skins of partially developed silver bromide crystals (notice etch-depressions).

a.

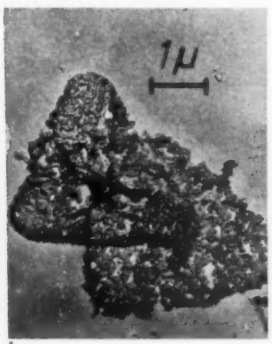

b.

c.

Fig. 7. Electronmicrographs of developed silver bromide crystals: a, direct exposure, active developer without silver halide solvent; b, image of carbon replica, active developer without silver halide solvent; c, image of carbon replica, developer of low activity with silver halide solvent.

by selective etching with the aid of solvents. Suitable solvents for the etching of silver halide crystals are silver complexing agents such as sulfite and cyanide ions. The effects of such agents on microcrystals of silver halides are observable in the four electronmicrographs of Fig. 3. It is clearly evident from Figs. 3a and 3b how crystallographically preferred etching planes are formed in pyramidal and flat, triangular crystals of silver bromide: the etching was carried out with sulfite and thiosulfate solutions which leads to the formation of $Ag(SO_3)_2^{---}$ and $Ag(S_2O_3)_3^{-5}$ complexes. Pyramids of silver iodide, on the other hand, exhibit preferential etching at the sides, probably because crystallographically the chances for step-formation are greater at the side than at the base plane [base plane $(100\bar{0})$, side planes $(1\bar{1}10)$, with permutation of the last three indices].

3. *Structural details of the developed silver.* The carbon-replica technique has been applied also in the study of photographic development processes.[5] Jaenicke,[6,7] Mitchell[8] and others have postulated that development proceeds by electrode processes (short-circuit element) in that the latent image silver speck acts as an anode and accepts electrons from the developer solution where it is in contact with it. The silver speck-crystal interface, on the other hand, acts as cathode and the discharge of silver ions at this site constitutes the cathodic current. In chemical development these silver ions are donated exclusively by the silver halide crystal and a silver filament is formed at the interface through continuous, new formation of silver.

It was possible to prove through judiciously interrupted development of a silver bromide grain that silver ions can migrate to the latent image speck over great crystal distances (Fig. 4), and that zones of imperfect crystal structure are depleted preferentially. The three cavities that may be seen in Fig. 4, spaced 120 degrees apart, equal in silver bromide volume that of the silver filament that is discernible at the right of the grain. The equivalent silver bromide volume of the silver filament could be computed from measurements made on a stereo-electronmicrograph.[9]

Additional examples of results obtained with interrupted development are shown in Figs. 5 and 6. It is evident from these that the silver halide grain may also be dissolved in the immediate vicinity of the developing site but that crystallographically preferred directions are followed in the dissolution (Fig. 6). In all of these examples, a developer without silver halide solvent was used.

Partial physical development occurs when the

developer contains silver halide solvents, i.e., silver ions are donated by the developer solution and are reduced at the previously formed silver specks. As might be expected, this alters the detail structure of the developed silver.

The differences between solvent-free and solvent-containing development are illustrated in Fig. 7. Silver grains developed in a solvent-free developer are shown in Figs. 7a and 7b, the former photographed directly in the electron microscope, the latter by means of the carbon-replica technique. (The compact form of the grain seen in Fig. 7a is not always maintained and loose filaments develop under some conditions.) The results of development of silver halide grains of equal composition in a developer that effects partial physical development are depicted in Fig. 7c. Here again the carbon-replica technique was employed.

It has been the purpose of this paper to report on new, experimental results of investigations carried out with the electron microscope without consideration of the theoretical evaluations. It will be evident, however, that a host of other problems in this field may be studied with the method described.

References

1. Klein, E., *Mitt. Agfa Leverkusen* (Muenchen), Vol. 1, p. 10 (1956).
2. Klein, E., *Phot. Korr.*, Vol. 91, p. 179 (1955).
3. Bradley, D. E., *J. Appl. Phys. B.*, Vol. 3, p. 96 (1954).
4. Mees, C. E. K., *The Theory of the Photographic Process*. The Macmillan Co., New York, N.Y. (1942).
5. Klein, E., *Z. f. Elektrochemie*, Vol. 60, p. 998 (1956).
6. Jaenicke, W., et al., *Z. Phys. Chem.*, Vol. 197, p. 161 (1951).
7. Jaenicke, W., and Schott, C., *Z. f. Elektrochemie*, Vol. 59, p. 956 (1955).
8. Keith, H. D., and Mitchell, J. W., *Phil. Mag.*, Vol. 44, p. 877 (1953).
9. Evans, T., and Mitchell, J. W., *Report on Bristol Conference*. J. Buttersworth & Son, London (1954), p. 409.

PHOTOGRAPHIC SCIENCE AND ENGINEERING
Volume 1, Number 2, October 1957

Effects of Some Organic Compounds on Zeta-Potential of Silver Bromide

SHIN SUZUKI AND YASUSHI OISHI, *Department of Applied Chemistry, Faculty of Engineering, University of Tokyo, Japan*

The electrophoretic behavior of silver bromide sol has been studied. At pH 6 and pAg 9, the sol has a zeta-potential of −55mv and is stable. On the addition of small quantities of thiourea and benzimidazole to the acidic sol, remarkable changes in the zeta-potential and stability are found to occur; on increasing the addition quantity of the organic compounds, the zeta-potential of silver bromide changes from −55mv to 60mv for thiourea, and to 40mv for benzimidazole. Both on the negative and the positive sides, the sol is fairly stable, but near the isoelectric point it flocculates promptly. In the basic sol, however, such a reversal of zeta-potential does not occur. Urea and 6-nitrobenzimidazole do not change the potential. The shift of zeta-potential by thiourea and benzimidazole is attributed to their adsorption on silver bromide surface in ionized forms (as cations).

Detailed studies of the electrophoretic behavior of silver bromide in aqueous inorganic electrolytes have been made by several workers,[1,2,3] but knowledge of the effects of organic compounds on the electrokinetic behavior of silver bromide is rather poor.

Indra[4] measured the electrophoretic mobility of silver halides in the presence of fluorescein dyes, whereas Chandhury[5] investigated the effects of adsorption indicators on silver bromide surface by electrophoresis. Holliday and Davies[2] studied the effect of methylene blue and sodium fluoresceinate on electrophoretic mobility of silver bromide in the presence of excess silver ion.

The changes of electrokinetic potential (zeta-potential) brought about by the added organic compounds are attributed to the adsorption of the organic ions. The direction of shift of potential, therefore, indicates the electrical states of adsorbed compounds on the silver bromide surface.

The organic compounds examined in this study are: thiourea (chemical sensitizer), urea, and benzimidazoles (antifoggants).

Experimental Procedure

In this study, a moving boundary electrophoretic apparatus was used to determine the electrophoretic mobilities of silver bromide sols (Fig. 1). The electrophoresis was carried out under the electric potential gradient of 5.20 volts per centimeter for 15 minutes at 12 C.

The silver bromide sols were prepared by pouring 0.1*N* silver nitrate solution into a potassium bromide solution containing 4 per cent excess bromide with mechanical stirring. The sols were left to stand for 20 hours and were diluted after the addition of saccharose. The composition of the final sol was:

AgBr.....2×10^{-3} mol solid AgBr per 1 l sol
KNO_3.....2×10^{-3} M
Saccharose.....2%

The desired pH values were obtained by adding

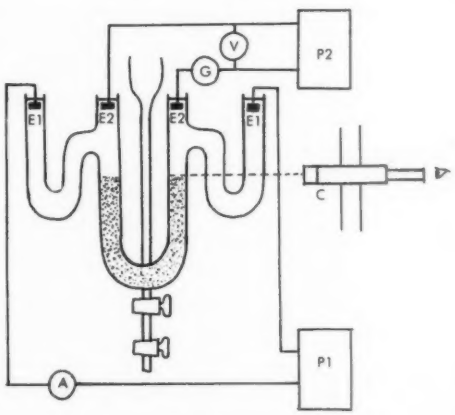

Fig. 1. Electrophoretic apparatus.

E1—main electrodes for applying electric field
E2—Electrodes for determining electric potential gradient
A—Ammeter
G—Galvanometer
V—Voltmeter
P1, P2—DC source
C—Cathetometer

Read by Dr. Walter Cooper, Kodak Research Laboratories, Eastman Kodak Company, Rochester, N.Y., at the Annual Conference, Asbury Park, N. J., 12 September 1957. Received 15 August 1957.

solutions of nitric acid, sodium hydroxide or borax, and the desired pAg values by the addition of silver nitrate or potassium bromide. The solutions of known concentration of thiourea or other organic compounds were added to the sol. The specific surface area of silver bromide was 2.5×10^5 cm^2/g AgBr as measured by the adsorption of 1,1′-diethyl-2,2′-cyanine iodide. The addition of saccharose tended to form sharp boundaries.*

The zeta-potential is given by

$$\zeta = \frac{1}{f(\kappa a)} \cdot \frac{4\pi\eta}{D} \cdot m$$

where ζ is the zeta-potential; $f(\kappa a)$ the Henry's factor; η the coefficient of viscosity of the medium; D the dielectric constant of the medium; and m the electrophoretic mobility.

Results and Discussion

The zeta-potentials of silver bromide were measured at various pH and pAg values (Figs. 2 and 3). In the presence of excess silver ion or bromide ion, the sols were stable. Near the isoelectric point, however, they were unstable and therefore an accurate determination of mobility values was impossible.

In acidic sols containing excess bromide, the addition of a small quantity of thiourea resulted in a remarkable change in the zeta-potential and in the stability of the silver bromide sol. The proper silver bromide sols had a zeta-potential of −55 mv and were stable. With the addition of 4×10^{-3} mol thiourea/mol AgBr, the sol had no net charge and flocculated promptly but with the addition of 4×10^{-2} or more, the potential attained the constant value of +60 mv and the sols were fairly stable (Fig. 4). Both in acidic sols containing excess silver nitrate and in alkaline sols containing excess bromide, no changes in zeta-potential were observed, but the sols were colored brown. This coloration is probably due to the formation of silver sulfide on the silver bromide particle surface, as shown by James.[6]

$$2AgBr + NH_2{-}\underset{\underset{S}{\|}}{C}{-}NH_2 \rightarrow Ag_2S + NH_2{-}C{\equiv}N + 2HBr$$

The silver bromide sols treated with sodium sulfide were brown and were found to have the same zeta-potential as silver bromide sols.

The shift of zeta-potential by thiourea at low pH and high pAg indicates that there are excess positive charges on the silver bromide surface. This is attributed to the adsorption of thiourea in the following ionized form (as cation):[7]

$$NH_2{-}\underset{\underset{S}{\|}}{C}{-}NH_2 + H_2O \rightleftarrows NH_2{-}\underset{\underset{S}{\|}}{C}{-}NH_3^+ + OH^- \quad pK_a = -1.0$$

The effects of the addition of urea on zeta-potential were studied also but no changes were observed.

Similar measurements were carried out with benzimidazole and 6-nitrobenzimidazole but only in the presence of excess bromide (Fig. 5).

In alkaline sols, benzimidazole caused a reversal of zeta-potential, but it was noticed that a much larger quantity of benzimidazole (2.0×10^{-1} mol/mol AgBr) than of thiourea was required to secure the re-

* The chemicals used in this study were of highest purity.

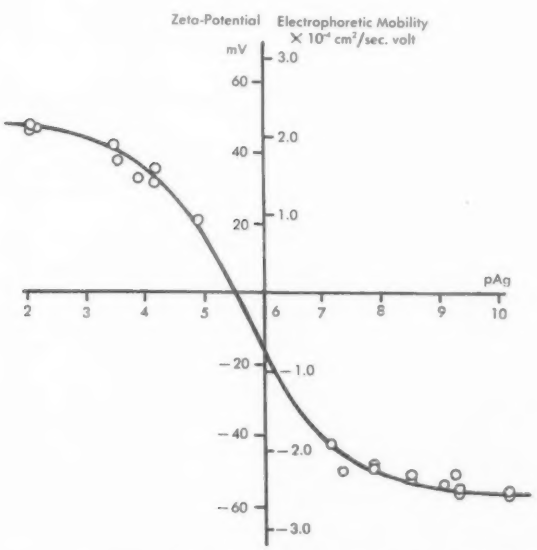

Fig. 2. Zeta-potentials of silver bromide at various pAg values. (pH 5.5–6.0).

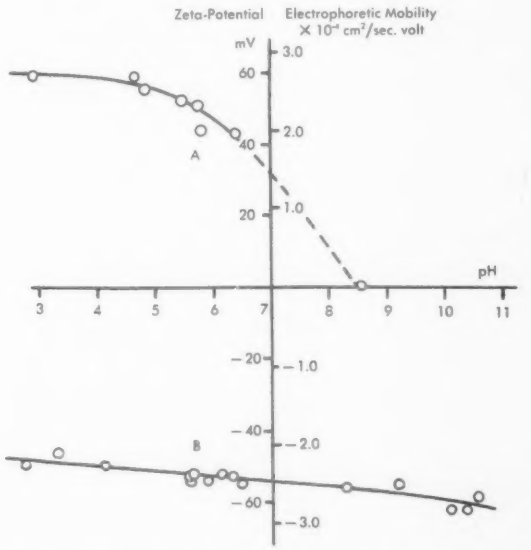

Fig. 3. Zeta-potentials of silver bromide at various pH values. Curve A—pAg 2.5 Curve B—pAg 9.0

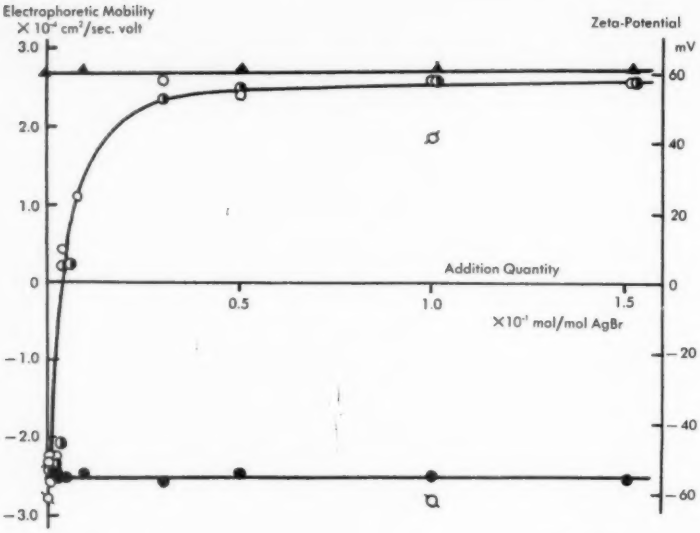

Fig. 4. Effect of thiourea on zeta-potential of silver bromide.

pH 3, 6, 7, 9, 10 } pAg 9.0 ▲ pH 3, pAg 2.5

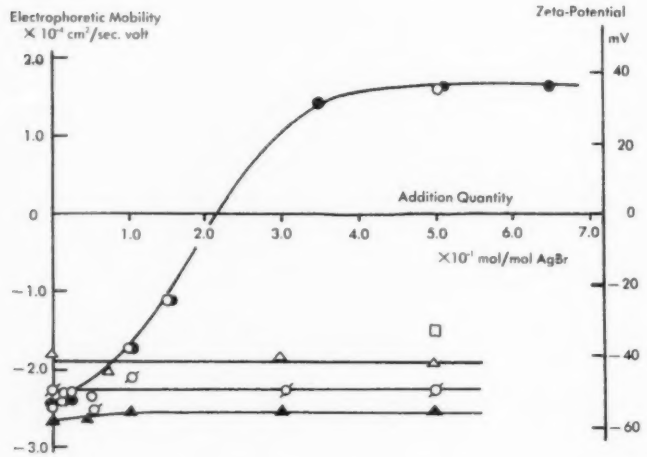

Fig. 5. Effect of benzimidazoles on zeta-potential of silver bromide.

Benzimidazole

pH 3, 5, 7, 9 } pAg 8.5

6-Nitrobenzimidazole

pH 8.5, 10.5 } pAg 11.0

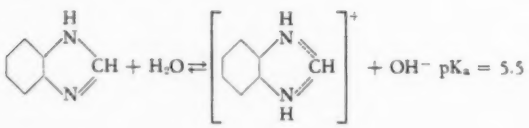

versal of potential. This reversal of potential also is attributed to the adsorption of ionized benzimidazole.[8]

Neither benzimidazole in acidic sols nor 6-nitrobenzimidazole changed the zeta-potential of silver bromide.

The authors wish to express their appreciation to Prof. S. Oka for his guidance.

References

1. Kolthoff, Reyerson, and Coad, *J. Phys. Chem.*, Vol. 51, p. 321 (1947).
2. Holliday and Davies, in *Fundamental Mechanism of Photographic Sensitivity*, ed. Mitchell, p. 56. London (1951).
3. Davies and Holliday, *Trans. Faraday Soc.*, Vol. 48, p. 1061 (1952).
4. Indra, *J. Ind. Chem. Soc.*, Vol. 16, p. 15 (1939).
5. Chandhury, *J. Proc. Inst. Chem. India*, Vol. 13, p. 1 (1941). [C. A., Vol. 36, p. 4771 (1942)].
6. James, *J. Phys. Chem.*, Vol. 57, p. 725 (1953).
——, *J. Phot. Sci.*, Vol. 1, p. 133 (1953).
7. Scudder, in *Electrical Conductivity and Ionization Constants of Organic Compounds*, p. 295. London (1912).
8. Hafman, in *Imidazoles and its Derivatives*, Vol. 1. New York (1950).

PHOTOGRAPHIC SCIENCE AND ENGINEERING
Volume 1, Number 2, October 1957

Control of Low-Intensity Reciprocity Law Failure with Mercaptooxazoline Development Retarders

ERNEST T. LARSON AND HAROLD A. LEVINE, *Research Laboratories, Ansco, Binghamton, N.Y.*

A new class of development retarders, the 2-mercaptooxazolines, minimize low-intensity reciprocity law failure. They may be used for this purpose with radiation dosimeters that consist of photographic film and fluorescent screens. The sensitometric effects of the new compounds in developers are described. Control of reciprocity failure by development retarders is explained in terms of the slower developability of latent image formed at moderate and high exposure intensities.

A single sample of a normal radiographic film cannot be used to measure the accumulated exposure of a subject to heterogeneous x-ray radiations, because its response is wavelength dependent. The film is about 25 times more sensitive to 65-kilovolt x-ray radiation than to 1-million-volt x-ray radiation. This wavelength dependence can be nearly eliminated by placing an appropriate fluorescent screen against the film. The light emission of the fluorescent screen is greatest for high-energy radiation and least for low-energy radiation. Since the film is least sensitive to high energy quanta, the response of the fluorescent screen compensates for the lack of film sensitivity. The result is approximate wavelength independence over the energy range for which the film might be used as a radiation dosimeter.

The use of both light and x-radiation, however, introduces another problem, reciprocity law failure. It is known that the reciprocity law holds for exposures to x-rays, but when a film is exposed to a given amount of low-intensity light, less density usually develops than when it is exposed to the same amount of light energy at high intensity. This is known as low-intensity reciprocity law failure.

A typical response curve of a film exposed to visible light over a range of low intensities is shown in Fig. 1. In this plot, a horizontal straight line would represent the response of a film without reciprocity failure. Actually more than four times the exposure is needed at 40 hours than at 1 second to yield a net developed density of 0.40.

Accurate monitoring of radiation exposures requires that the developed density be the same for equal total exposures, whether the exposure time is 1 second or 40 hours. In other words, the developed density on the film should be the same for exposures to low-intensity continuous radiation, intermittent radiation, or high-intensity short duration energy bursts.

A method for obtaining a nearly flat response over the time and intensity range to which a dosimeter film may be exposed involves the principle of retarded development. By preferentially suppressing or retarding the developability of the normally exposed latent image, low-intensity failure may be masked effectively. A certain amount of the response at the 1-second exposure level is deliberately sacrificed in order to approximate uniformity across the intensity range. This is done by adding substances such as 6-nitrobenzimidazole (6-NBA) or 1-phenyl-5-mercaptotetrazole to the developer.

The principles of film dosimetry using a fluorescent screen and development retardation were demonstrated

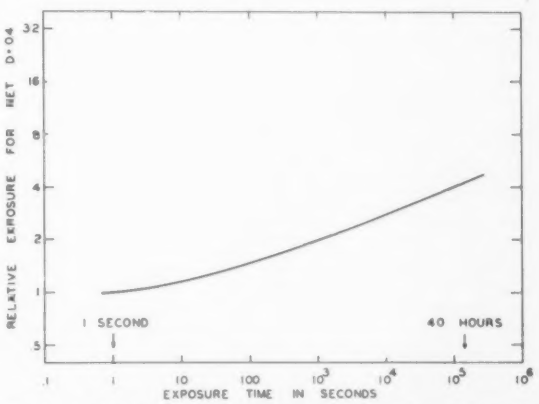

Fig. 1. Typical response curve of film exposed to visible light over a range of intensities.

Presented at the 1957 Annual Conference, Asbury Park, N.J., 12 September 1957. Received 28 August 1957.

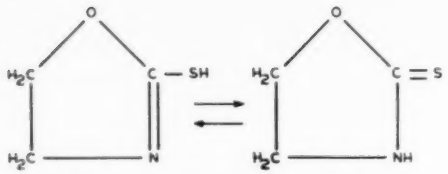

Fig. 2. Structure of 2-mercaptooxazoline (SHOX).

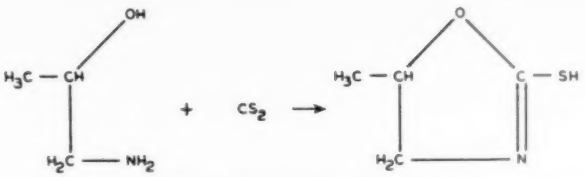

Fig. 3. Synthesis of 5-methyl-2-mercaptooxazoline (5-methyl-SHOX) from 1-amino-2-propanol and carbon disulfide.

by H. Hoerlin, R. H. Clark, D. P. Jones, F. J. Kaszuba, and E. T. Larson of these laboratories.[1] The work reported here is the outgrowth of a search for superior development retarding substances. This search was guided by the following criteria:

1. *Correction of Low Intensity Failure*
   The exposure needed to produce the 0.40 density at 40 hours time should be no more than twice that required at 1 second.
2. *Low Fog*
   The developed density in the unexposed areas of the film should be low. The retarder should be an antifoggant.
3. *Satisfactory Speed*
   The retarder should exert its effect without too great a loss in film speed.
4. *Solubility*
   The retarder should be sufficiently soluble in water or in developer to allow use either in a prebath or in the developer.
5. *Availability*
   The retarder should be inexpensive and readily available.

Certain 2-mercaptooxazolines (SHOX) that are members of a newly discovered class of antifoggant development retarders met the outlined requirements sufficiently well to be of interest. The parent structure of these simple heterocyclic compounds is illustrated in Fig. 2. Members of this class of compounds are readily synthesized from 1,2-aminoalcohols, such as ethanolamine or propanolamine, by reaction with carbon disulfide (Fig. 3).

Experimental Results

The effectiveness of these compounds in reducing low-intensity reciprocity failure when added to a developer was evaluated with the aid of a commercially available, prepared x-ray developer and a high-speed, negative type film (Fig. 4). It will be noted that use of the mercaptooxazoline brought about a flattening of the reciprocity-failure curve as well as a loss in effective film speed. The values of fog, speed, and the effects of the mercaptooxazolines on reciprocity failure are summarized in Table I.

In this table the speed values are calculated relative to the speed at the 1-second exposure time level. Reciprocity failure is expressed in terms of full lens stops and represents the maximum difference in exposure required between the 1-second and the 40-hour exposure time levels to yield a net density of 0.40.

The concentration of the retarder is given in milligrams per liter of developer. The data show that the SHOX development retarders reduce the reciprocity-failure range of this film to one f/stop or less. The film speed at the 1-second level is about one-fifth of its original value and fog is brought to an acceptable level.

A comparison of other known retarders and mercaptooxazoline is given in Table II.

As can be seen, mercaptooxazoline produces a somewhat smaller reciprocity failure range than other retarders at essentially the same speed level. Further, good water solubility, ready availability, and acceptable control of fog qualify mercaptooxazolines for use in radiation film dosimetry.

Mechanism of the Retarder Action

The retarding properties of the mercaptooxazolines were studied in order to gain insight into the mechanism whereby development retarders affect low-intensity reciprocity law failure. A high-speed negative film characterized by a marked tendency to fog on

TABLE I
Reciprocity Failure Activity of SHOX Development Retarders

Retarder	Fog	Relative Speed	Reciprocity Failure (f/stops)	mg/l
None	0.32	100	2.2	—
SHOX	0.09	18	1.0	130
5-methyl SHOX	0.08	19	0.9	90
4-ethyl SHOX	0.09	21	0.9	70

TABLE II
Reciprocity Failure Activity of Development Retarders

Retarder	Fog	Relative Speed	Reciprocity Failure (f/stops)	mg/l
None	0 32	100	2.2	—
SHOX	0.09	18	1.0	130
6-NBA	0.08	15	1.4	1100
1-phenyl-5-SH-tetrazole	0.09	17	1.1	130

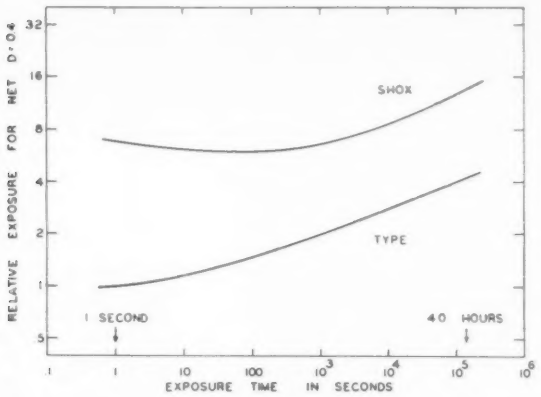

Fig. 4. Reciprocity failure curves for film developed for 3 minutes in a conventional developer and in the same type of developer with SHOX added. Reciprocity failure measured as maximum difference in exposure values between 1 second and 40 hours.

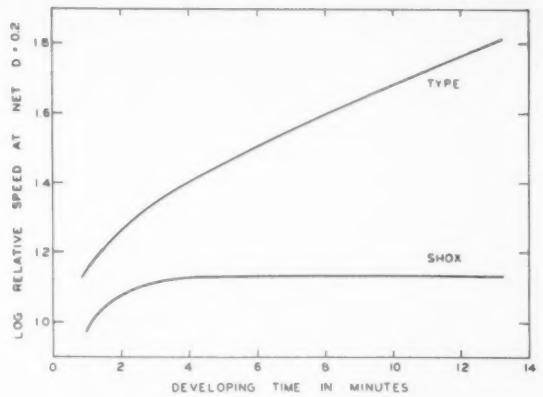

Fig. 5. Curves showing relative speed of film developed to net density of 0.2 in a conventional developer and in one containing SHOX for a range of developing times.

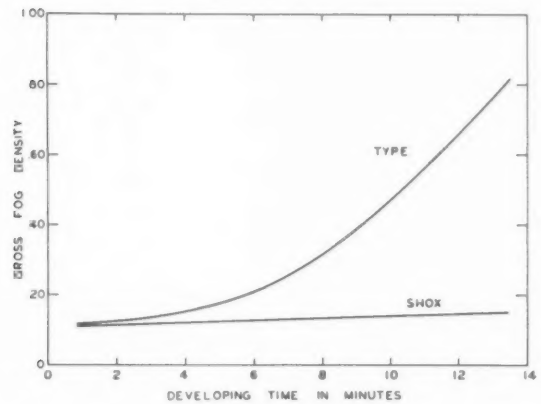

Fig. 6. Growth of fog with development time curves for film developed in a conventional developer and in one containing SHOX.

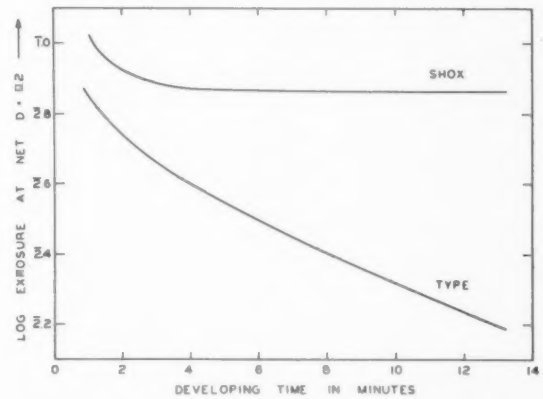

Fig. 7. Exposure required to produce a net density of 0.2 at various developing times in a conventional developer and in one containing SHOX.

prolonged development was used for these tests. Exposure time was 4 minutes and development was carried out in a highly alkaline, metol-hydroquinone developer. A comparison of the changes in film speed obtained with changes in development time is given in Fig. 5 for development with and without 100 mg of SHOX per liter of developer.

The speed of the normally developed material increased continually with increasing development, whereas the film speed in retarded development remained essentially constant over a wide range of times. The corresponding fog versus development-time curves (Fig. 6) show that the fog of normally processed film increased at an accelerating rate as development proceeded, whereas in the SHOX retarded developer good control of development of fog was obtained.

The data of Fig. 5 were replotted (Fig. 7) to correlate the exposure required to produce a density of 0.2 with development time. These curves are typical of results obtained at higher densities.

Inspection of the "type" development curve reveals that at 6 minutes development about one half as much exposure is needed as at 2 minutes development to obtain a density of 0.2. Thus, increased exposure increased the rate of development of the layer in the normal developer, i.e., more light energy resulted in a more rapid formation of density. The additional exposure altered some of the crystals so that they developed faster. This would be true whether the additional exposure increased the number of crystals which developed or produced a greater developed size from the original developing crystals.

During retarded development, however, increased exposure did not substantially affect development rate for developing times of more than 3 minutes. Apparently, the retarder sets an upper limit to the rate at which the crystals can develop, regardless of how much exposure the layer receives. The maximum rate of development is considerably less than for the normally processed layer.

It appears that developer retarders such as the mercaptooxazolines effectively prevent the development of some of the latent image which would normally develop. Since both the speed and the fog density reach nearly maximum values in retarded development within very short development times, the retarding action probably is most effective for crystals that have a slow-developing latent image.

These observations are consistent with the assumption that the reduction of low-intensity reciprocity failure by developer retardation is based on the differences in developability of the latent images formed at high and at low intensities. Berg[2,3] showed that the density produced by a low-intensity exposure to light develops more rapidly than that produced by a high-intensity exposure. Therefore, reducing the developing time or weakening the developer would be expected to favor the development of the low-intensity image relative to the high-intensity image. Chemical retardation of development is a practical way of achieving the same result. James[4] has stated that all antifoggants decrease the rate of development of the latent image.

It may be postulated, therefore, that a development retarder decreases low-intensity failure by preventing the development of some of the slowly developable latent image formed at normal intensities. Latent image formed at high intensity is more susceptible to the action of the retarder because it inherently has a lower developing rate. In other words, a larger fraction of the high-intensity image is rendered nondevelopable. The photographic speed loss which occurs over the entire range of intensities is greatest in the high-intensity exposure region and, as a result, there is a marked reduction in low-intensity reciprocity law failure.

References

1. Hoerlin, H., Clark, R. H., Jones, D. P., Kaszuba, F. J., and Larson, E. T., *Development of a Wavelength—Independent Radiation Monitoring Film*. Argonne National Laboratory Final Report 5168 (1953).
2. Berg, W., *Sci. et Ind. Phot.*, Vol. 20, p. 401 (1949).
3. ——, *The Theory of the Photographic Process*, ed. C. E. K. Mees, Revised ed. The Macmillan Co., New York (1954), p. 220.
4. James, T. H., *ibid.*, p. 678.

PHOTOGRAPHIC SCIENCE AND ENGINEERING
Volume 1, Number 2, October 1957

Wedge Brittleness Test for Photographic Film

P. Z. ADELSTEIN, *Manufacturing Experiments Division, Eastman Kodak Company, Rochester, N.Y.*

The brittleness of photographic film is difficult to evaluate quantitatively, due in part to the different types of brittle failure. The Wedge Brittleness Test uses a simple inexpensive apparatus to measure film brittleness. It not only gives the brittleness level, but subsequent examination of the samples gives information about the type of break. The test is reproducible and is a useful tool in this field. Experimental data are given which show the effects of relative humidity, emulsion-support adhesion, support thickness, and emulsion thickness on film brittleness.

The ability to characterize the brittleness of a given piece of photographic film is extremely important in the technology of the film industry. While photographic films are quite flexible at moderate and high relative humidities, they generally show brittle behaviour at low relative humidities. This low-humidity brittleness varies with different films and is influenced by the physical composition of the film laminate. Yet of all the physical properties of film that are of practical importance, brittleness is one of the most difficult to determine quantitatively and reproducibly. Different film products are used in different ways and the type of brittle failure which is observed in graphic arts films, for example, can be very different from that which occurs in motion picture films. Therefore, the film technologist must devise a brittleness test in the laboratory which can accurately determine how a material behaves under a host of different conditions.

Photographic film can show a wide variety of brittle failures because of its very complex physical make-up. A brief consideration of the essential components of photographic film illustrates this point. Film consists of an 0.003 to 0.010-inch plastic support or base which is coated with one or more water-permeable layers making up the light-sensitive photographic emulsions. These emulsion layers usually contain gelatin as the carrier for the silver halide and may vary between 0.0002 and 0.0013 inch in thickness. In addition, photographic films have "sub" layers which bind the emulsion to the plastic support, and many films have antihalation layers, antiabrasion layers, or static protection coatings which can be as thin as 0.00002 inch.

The most common type of brittle failure in photographic film is a complete break of both the emulsion layers and the support. Frequently, however, photographic film shows a cracking of the emulsion layer with no damage to the support. Cases have also been observed where brittleness is the result of a crazing or cracking of the plastic base which can initiate a rupture of the emulsion layer. Therefore, a satisfactory brittleness test should not only be capable of measuring the level at which failure occurs, but also give an indication of the type of failure. This latter information can frequently be as important as the brittleness level of the product.

In addition, a test should be simple to perform, give reproducible and meaningful results, and have a large numerical range over the complete scale of film brittleness.

To date there have been several tests used to evaluate film brittleness, but each has disadvantages. One type of test is a folding endurance test in which a sample is folded back and forth until it breaks and the number of folds counted. This is a fatigue test, not a shock test. The Pfund Folding Endurance Test is specified in the American Standard Specification for Films for Permanent Records.[1] This is a manual test, however, and is very laborious to perform. Furthermore, its reproducibility is poor and it only gives the number of folds at which a complete break occurs in the sample. No information is given about the occurrence of any emulsion cracks or support crazing.

An improvement over the Pfund tester is the MIT Folding Endurance Tester.[2] This apparatus was originally designed for paper but has since been found applicable for photographic film. It is an automatic testing machine and gives better reproducibility than the Pfund tester. Like any folding test, however, it only gives the number of folds to complete break of the sample. Misleading results can be obtained if emulsion cracking or peeling occurs at the folded area during the test, with a subsequent flexing of the support alone. In such cases the folding endurance of the base is recorded and not that of the film laminate.

A more common test for film is the Vise Brittleness Test[3] which is used in military specifications.[4] Small loops of film, bent emulsion-side out, are placed between the jaws of a vise which are closed at a constant speed of 0.017 inch per second. When the sample cracks, the vise is stopped and the distance between the jaws is taken as a measure of the film

Presented at the Annual Conference, Asbury Park, N.J., 10 September 1957. Received 3 January 1957.

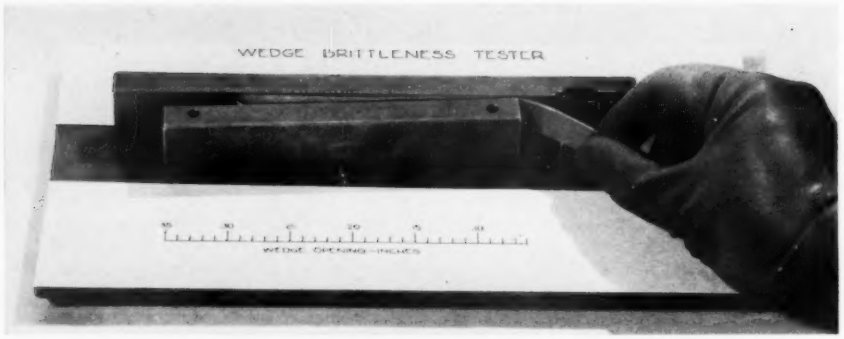

Fig. 1. The Wedge Brittleness Tester.

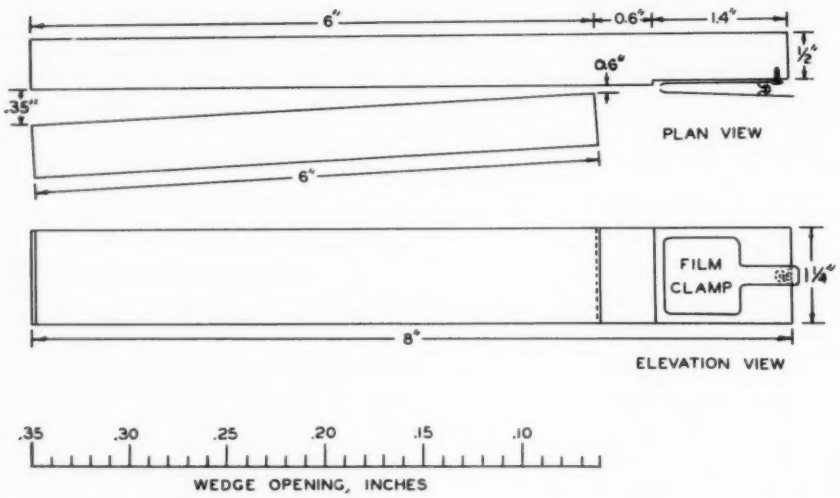

Fig. 2. Plan and elevation views of the Wedge Brittleness Tester.

brittleness. Sample breaks or cracks are determined visually or audibly, at the instant they occur, but frequently fine emulsion cracks are missed. Efforts to facilitate the determination of the end point of this test with a crystal cartridge to detect the vibrations caused by emulsion cracking have been of some help. In addition to this difficulty, the observed brittleness scale in the Vise Brittleness Test is compressed. Frequently, films of moderate brittleness give only very low vise openings.

It is therefore apparent that there has been a real need for major improvements in the existing tests or for a completely new brittleness test. For many years extensive work has been done in this field, as a result of which the Wedge Brittleness Test was developed. While it has some drawbacks, it contains many features which have proven quite useful in determining the brittleness characteristics of a wide variety of photographic films.

Apparatus

The Wedge Brittleness Test apparatus consists of two non-parallel metal plates or jaws which form a wedge or V (Figs. 1 and 2). One end of a 12-inch by 15mm film sample is fastened in the clamp at the narrow opening of the wedge. The sample is looped, emulsion side out, through the wedge with the other end of the sample protruding through the narrow opening. This end is rapidly pulled through the narrow wedge opening by hand. The wedge separation (which can be considered as roughly the diameter of curvature at which the film shows failure) is taken as the measure of brittleness. This is the same criterion as is used in the Vise Brittleness Test,[3] but the action of the film is quite different.

As the film loop is pulled through the wedge, the film area being tested is constantly changing. Thus a much larger sample area is being effectively tested than if only a small area of the film were bent. This should lead to a greater uniformity of results, and is considered one of the principal advantages of this test.

Another important advantage of this test is that it is not necessary to pull the film through the wedge slowly in order to observe at what wedge separation failure occurs. The procedure adopted is to draw a pencil line on the film sample at the point where the wedge starts. After the sample has been broken, the

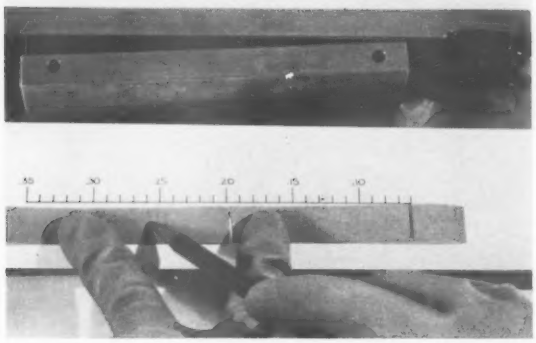

Fig. 3. Determination of brittleness values from film sample broken in Wedge Brittleness Tester. Emulsion crack value is 0.26 inch and film break is 0.20 inch.

distance from this pencil mark to the broken end of the sample is measured and this is directly proportional to the wedge opening at failure. A scale is used in which this sample length can be converted directly into wedge separation (Fig. 3).

With many materials, failure is first observed as emulsion cracking, followed by a complete film break at a lower wedge separation. In such instances, it is important to obtain the wedge separation for the first emulsion crack as well as for the complete film break. These values can be obtained from the broken film sample as shown in Fig. 3, by examining both halves of the sample.

In reporting wedge brittleness results, it has been customary to report the average wedge opening for both emulsion cracks and complete film breaks. Frequently, however, some of the specimens of a material will show both cracks and breaks, while the remaining samples show breaks only. In such cases, a "first failure" value is calculated by averaging the observed emulsion crack values along with the film break values when emulsion cracks are not obtained.

Samples which pass through the narrowest part of the wedge (0.06 inch) without failure are assigned an arbitrary value of 0.04 to permit averaging. The percentage of samples which shows this behavior is also given.

An average first failure value of 0.10 inch or less represents a flexible film under the testing conditions employed, while a value of 0.25 inch or greater is considered a brittle film.

Testing Variables

There are several variables in this test which should be controlled, as follows:

a. Testing Speed. The testing speed in the wedge has been standardized so that a film loop is pulled through the wedge in approximately one second. Higher testing speeds give slightly higher brittleness results, as shown in Fig. 4 for testing times ranging from $^1/_3$ to 6 seconds. Over this range, however, the variable is of secondary importance.

Since the rate of strain has a minor effect within the range studied, the angle of the wedge opening would not be expected to be too critical. This was verified experimentally. While a wider angled wedge increases the range of the instrument, it decreases the sensitivity. It was found that a maximum wedge opening of 0.35 inch is satisfactory for all but very brittle materials. Therefore, the normal wedge angle has been standardized according to the dimensions given in Fig. 2.

b. Sample Edges. As in many mechanical tests involving narrow-width samples, the results can be affected by the quality of the edges. Irregular or torn edges can cause premature failure and consequently erroneous results. This has been observed in the Wedge Brittleness Test.

c. Moisture Protection. Because gelatin is so strongly hydrophilic or moisture sensitive, the brittleness of photographic film is very dependent on its moisture content. All brittleness testing is therefore done under carefully controlled conditions of temperature and relative humidity, with the film samples completely equilibrated to the conditions chosen. It is also imperative that in brittleness testing at low relative humidity, the samples be protected from picking up moisture from the operator. The operator should wear rubber gloves. The importance of this procedure can be seen in Fig. 5, which shows that the use of cotton gloves is inadequate, resulting in poorer test reproducibility and in lower brittleness results.

Experimental Results

The reproducibility of the Wedge Brittleness Test has been found to be significantly better than that of

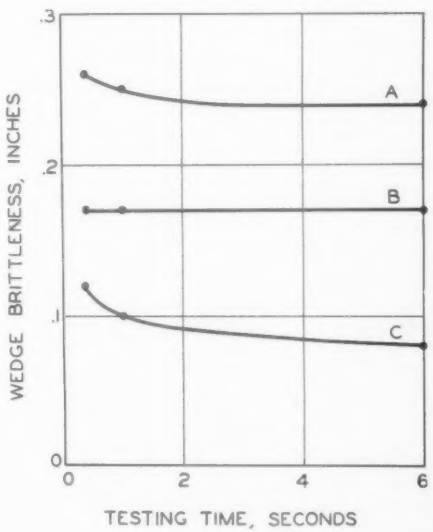

Fig. 4. Variation of wedge brittleness (first failure) with testing time for three experimental Kodachrome-type films at 70F-10% relative humidity.

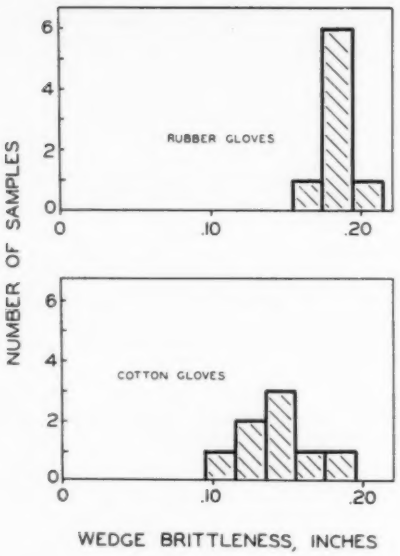

Fig. 5. Effect of wearing gloves on wedge brittleness (first failure) of experimental Kodachrome Film at 70F-10% relative humidity. Frequency distribution of average brittleness obtained by eight different operators. Fifteen samples tested by each operator.

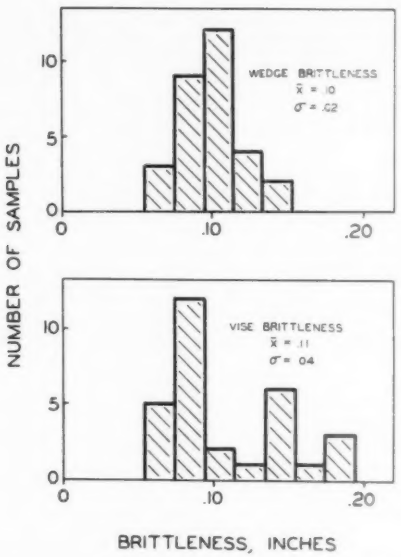

Fig. 6. Frequency distribution of brittleness of Ciné-Kodak-type film at 70F-10% relative humidity. Brittle failures are complete film breaks.

the other brittleness tests. This is shown by a comparison of the frequency distribution curves of the Vise and the Wedge Tests in Fig. 6. One of the factors responsible for the better reproducibility of the latter is believed to be the constantly changing area of film being tested. In the Vise Test, only a very small area of film is bent. Another reason for poorer reproducibility of the Vise Test is the greater difficulty of detecting emulsion cracks. (This does not apply to the results shown in Fig. 6, however, since the brittleness values represent complete film breaks in both tests.) Good correlations have frequently been obtained between the Vise and the Wedge Tests, with the latter showing a wider spread in numerical values between flexible and brittle films. When only poor correlations existed, the Vise Test has been suspect because of the difficulty in detecting emulsion cracks.

Excellent correlations have often been obtained between the Wedge Test and MIT Fold Test. However, it is believed that the different mechanical actions involved in the two tests contribute to the occasional lack of correlation. In fact, films on different supports have been ranked differently by the two tests. Any emulsion peeling at the folded area during the MIT test would also prevent good correlation.

The values of the Wedge Brittleness Test can be seen in quantitative data (Figs. 7–12) that show the influence of several factors on the brittleness of photographic film. The importance of relative humidity for three different types of film is demonstrated in Figs. 7, 8, and 9. Although the film brittleness (emulsion cracks) increases with decreasing humidity for all films, the shapes of the curves are quite different. The Kodak Verichrome-type film (Fig. 7) is much less dependent on humidity than the motion-picture positive-type film (Fig. 8). Moreover, with the Kodachrome-type film, the film break values continue to increase with decreasing humidity, whereas with the other two materials the values level off at the low humidities. These variations are due to differences in the chemical composition and physical structure of the films. It should be noted also that all these films are non-brittle at relative humidities above 30%.

Figure 10 shows the effect of emulsion-support adhesion in three experimental films in which the adhesion was intentionally varied. As the adhesion becomes poorer, cracking of the emulsion increases.

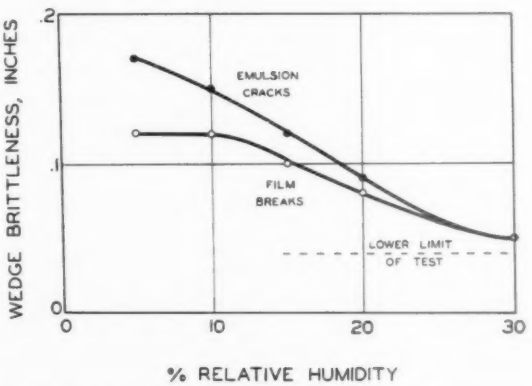

Fig. 7. Effect of relative humidity on wedge brittleness of Verichrome-type film.

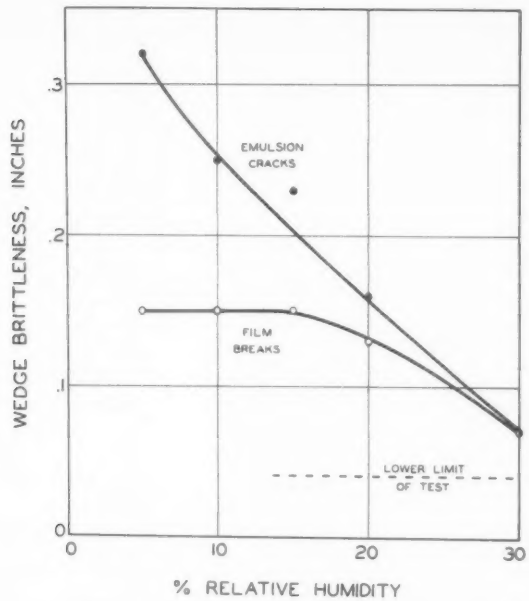

Fig. 8. Effect of relative humidity on wedge brittleness of motion-picture positive-type film.

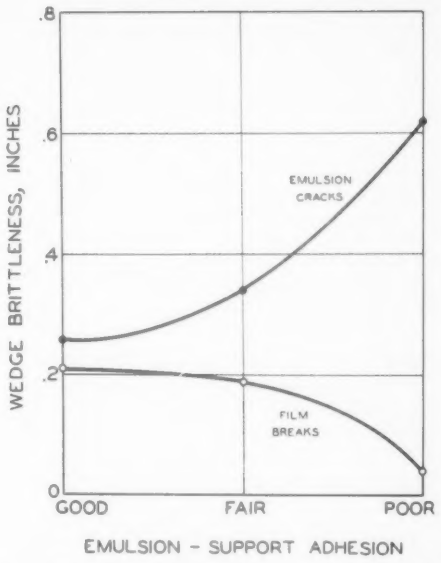

Fig. 10. Effect of emulsion-support adhesion on wedge brittleness of Verichrome-type film at 70F-15% relative humidity.

This is to be expected since the emulsion is the more brittle component of the laminate and is more prone to fail when it is weakly attached to the less brittle support. It should be pointed out also that as the adhesion becomes poorer, the emulsion cracks have much less tendency to propagate through the support and thus cause complete film breaks. Of course, in film manufacture the adhesion must be adequate and must be carefully controlled.

The effect of support thickness on film brittleness is shown in Fig. 11. A marked increase in wedge brittleness with increasing thickness would be expected since, as the thickness increases, the strain on the outside emulsion surface when bent increases directly, in accordance with the formula:

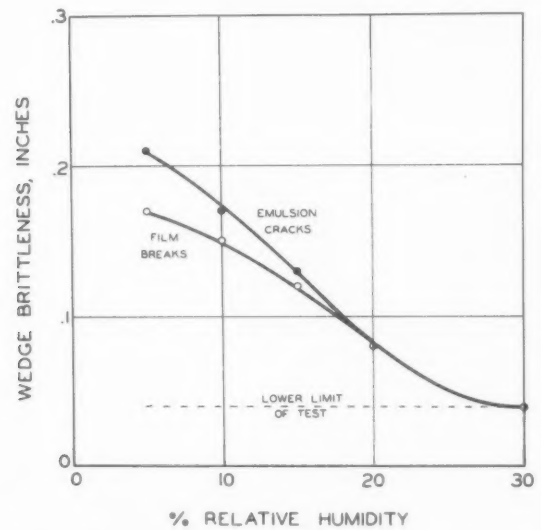

Fig. 9. Effect of relative humidity on wedge brittleness of Kodachrome-type film.

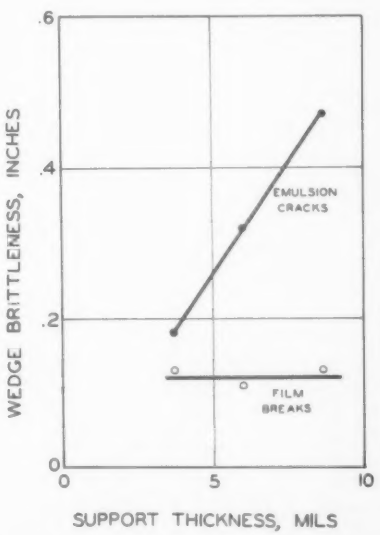

Fig. 11. Effect of support thickness on wedge brittleness of motion-picture negative-type film at 70F-10% relative humidity.

$$\% \text{ Strain} = \frac{t}{2R} \times 100,$$

where t is the total film thickness and R is the radius of curvature through which the film is bent.

As shown in Fig. 11, emulsion crack values increase with support thickness. Although film break values might also be expected to increase with thickness, this was not observed with these particular samples.

A marked increase in film brittleness with increases in the thickness of the photographic emulsion is shown in Fig. 12. Since the photographic emulsion is the most brittle component of the film laminate, this relationship is not surprising.

Conclusion

The Wedge Brittleness Test for measuring the brittleness of photographic film has the following advantages:

a. The apparatus is simple and inexpensive to build, and easy to operate.

b. The test has very good reproducibility.

c. The test gives valuable information about the type of film failure, in addition to the level of brittleness.

d. Considerable experience has shown that the results of this test are both reliable and meaningful.

It is not implied that the Wedge Brittleness Test is the complete answer to the evaluation of film brittleness. Because of the complicated nature of the problem, it is felt that several tests should be used to completely characterize this property. In such context, the Wedge Brittleness Test has a very useful place, and coupled with a folding test such as the M.I.T. Folding Endurance Test, a reasonably accurate appraisal of the brittleness of film can be made.

Acknowledgments

Acknowledgment is made to Dr. J. M. Calhoun and Dr. J. B. Hale, under whose direction this work was done, for their advice and many valuable suggestions. Thanks are also due to Messrs. E. J. Wiegand and E. K. Colton who furnished some of the experimental results.

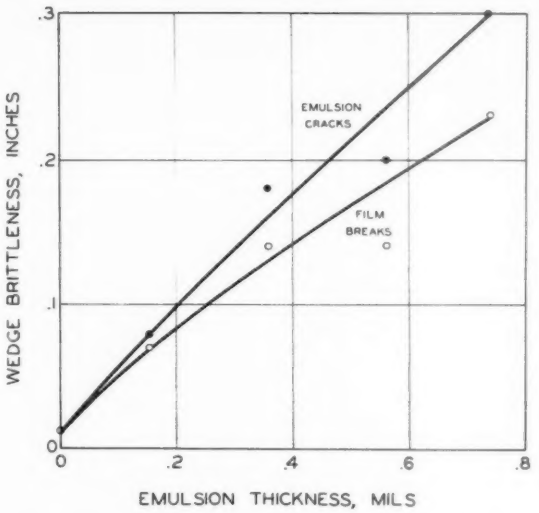

Fig. 12. Effect of emulsion thickness on wedge brittleness of motion-picture positive-type film at 70F-15% relative humidity.

References

1. "American Standard Specification for Films for Permanent Records," Z38.3.2-1945, American Standards Association, 70 E. 45th St., New York, N.Y.
2. Snyder, L. W., and Carson, F. T., *Paper Trade Jour.*, Vol. 96, No. 22, p. 40 (1933).
3. Calhoun, J. M., *Photogrammetric Eng.*, Vol. 13, p. 163 (1947).
4. United States Army-Navy Aeronautical Specification, "Film; Aerial Photographic," AN-F-40. 28 Aug. 1944, and Amendment-2, 19 Nov. 1945.

PHOTOGRAPHIC SCIENCE AND ENGINEERING
Volume 1, Number 2, October 1957

The Fundamental Nature of Curl and Shrinkage in Photographic Films

J. Q. UMBERGER, *Photo Products Department*,
E. I. du Pont de Nemours & Co., Inc., Parlin, N.J.

Manufacturers and users of photographic films are acquainted with dimensional changes which accompany changes in relative humidity. For example, cinematographic films that have a gelatin emulsion layer on one side of the support, only, curl into a circular arc when exposed to air of low relative humidity. The shrinkage of the emulsion exerts a bending moment on the base. Sheet films, such as portrait, lithographic, and radiographic products, usually have gelatin layers of equal thickness on each side of the support. Such films do not curl but instead shrink on exposure to dry air. The balanced gelatin layers exert no net bending moment on the film but rather a compressional stress.

With the objective of uncovering the basic nature of these humidity effects, curl and shrinkage data for various thicknesses of the support and the emulsion have been compared with equations derived by considering films as laminates of materials differing in moisture sensitivity. To a first approximation, curl is found to be directly proportional to the emulsion thickness and inversely proportional to the square of the base thickness. Film shrinkage is found to vary directly as the emulsion thickness and inversely as the first power of the base thickness.

During development of a new film base* with improved stability, concurrent studies were made of curl and shrinkage of coated films employing the base. The basic principles of beam bending appeared applicable to emulsion-base laminates and, in fact, have been used in the related case of bimetal thermostats.[1] Thus it was judged desirable to apply these principles to obtain quantitative correlation of curl and shrinkage with elastic moduli and shrinkage data obtained from independent measurements on component layers.

Experimental Curl Data

Film base which has a gelatin layer on one side, only, will curl into a circular arc when exposed to air of low relative humidity. The shrinkage of the gelatin layer exerts a bending moment on the film base. The radius of the resulting circular arc depends on the equilibrium between this bending moment and base stiffness or resistance to bending.

Curl data (Fig. 1) plotted for 4-mil film base as a function of gelatin coating weight, at various relative humidities at room temperature (70 to 80 F), show that curl is least for low coating thickness and at high relative humidity. However, when curl data are plotted for different thicknesses of film base with other variables held constant, it is noted that curl is least for thick film supports (Fig. 2).

In these graphs the curl has been expressed in "diopters," i.e., the reciprocal of the radius of curvature measured in meters. Film samples were cut 35 mm wide and about 10 inches long. After equilibration at the proper relative humidity (RH), the curl was measured by fitting arcs of known radius to the film samples. The curl data were averaged in such a way as to eliminate the effect of directional variations.

It is desirable to have a correlation of variables so that all the data of Figs. 1 and 2 can be presented on a single graph. This has been accomplished by comparison of the curled film to a bending beam, as outlined in Fig. 3. The data of Figs. 1 and 2 can now be fitted onto one "universal" plot, as shown in Fig. 4. From the theory described in Appendix A and from the above experimental data, it is seen that curl is proportional to the parameter θ. θ, as defined in Fig. 3, is a relatively simple function of the thicknesses, δ and Δ, and elastic constants, E′ and E, of the emulsion and the film base, respectively. It is noteworthy that essentially all the experimental points of Fig. 4 fall on a straight line passing through the origin. This is in accord with theory. The slope of this line is equal to 6β, where β is the linear coefficient of gelatin expansion with increase in relative humidity less the same coefficient for the support. From the data of Fig. 4, $\beta = 1.31 \times 10^{-4}$. The plotted points are surrounded by boundaries indicative of the magnitude of experimental errors.

Presented at the Annual Conference, Asbury Park, N.J., 10 September 1957. Received 21 August 1957.

* The data presented in this paper are for du Pont "Cronar" polyester photographic film base. The general principles outlined here, however, should apply to all types of supports and emulsions if allowance is made for differences in humidity coefficients and elastic moduli.

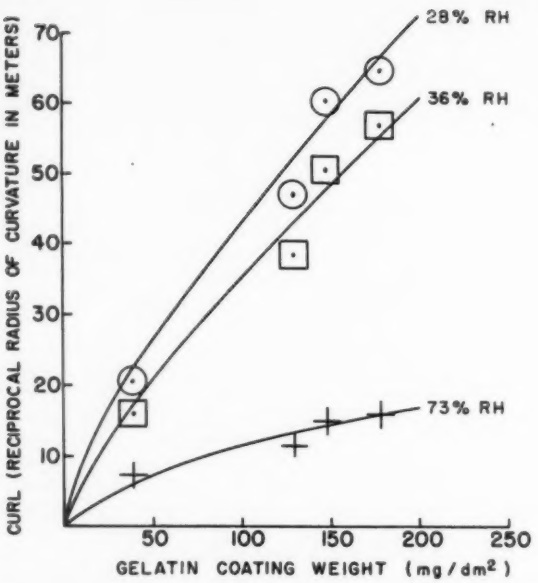

Fig. 1. Dependence of curl on gelatin coating weight and relative humidity (RH).
Thickness of base = 4.0 mils
Young's modulus of base = 5.3×10^5 lbs/in.²

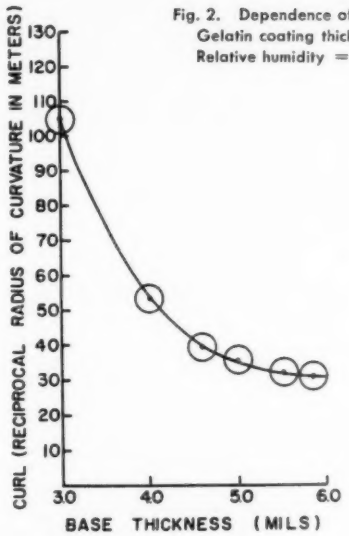

Fig. 2. Dependence of curl on base thickness
Gelatin coating thickness = 0.41 mils
Relative humidity = 25%

Experimental Shrinkage Data

Film base which has gelatin layers of equal thickness on each side will not curl but instead will exhibit a linear shrinkage when exposed to air of low relative humidity. The balanced shrinkages of the gelatin layers exert no net bending moment on the film base but rather a compressional stress. The amount of shrinkage of the laminate depends on the equilibrium between this stress and the compressional resistance of the base.

In Table I shrinkage data are listed for gelatin-coated film base of various thicknesses at 70 F:

TABLE I

Base Thickness Mils	Emulsion Thickness (on each side of base) mg anhydrous gelatin/dm²	Film Shrinkage Coefficient (fractional shrinkage for 1% RH decrease)	β
2.75	60	0.000033	0.00017
4.20	60	0.000020	0.00011
7.00	60	0.000015	0.00010
4.00	180	0.000041	0.00013
			0.00013

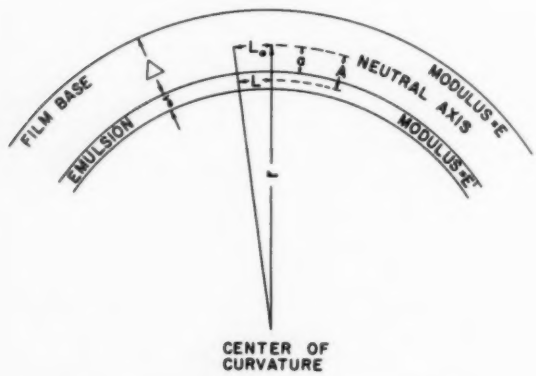

Fig. 3. Comparison of curled film to a bending beam.

Curl $\equiv \frac{1}{r} = 6\beta\theta$. θ depends on the thicknesses and elastic constants of the emulsion and the film base and β is the difference in the linear coefficients of expansion of gelatin and the support:

$$\theta = \frac{E'}{E}\frac{\delta}{\Delta^2}(100 - RH) \Big/ \left[1 + \frac{\delta}{\Delta}\left(4\frac{E'}{E} - 1\right)\right].$$

It is noted that film shrinkage is least for thick film base coated with a thin emulsion (gelatin).

The shrinkage coefficients in the third column of Table I were obtained by measurement of the film length at 70 per cent and 20 per cent relative humidity (RH). The fractional shrinkage divided by the per cent change in RH (70 − 20 = 50 per cent, in this case) equals the film shrinkage coefficient. The shrinkage coefficient was measured for duplicate samples cut at right angles to each other in order to eliminate directional variations.

It is again desirable to have a correlation of variables so that the data of Table I can be included in a single equation. This has been accomplished, as shown in Fig. 5. Here the film is represented as a laminate of relatively hydrophobic film base "sandwiched" between two thin hydrophilic emulsion (gelatin) layers. The equation relates film shrinkage with the thicknesses, δ and Δ, and the elastic constants, E′ and E, of the emulsion and the base, respec-

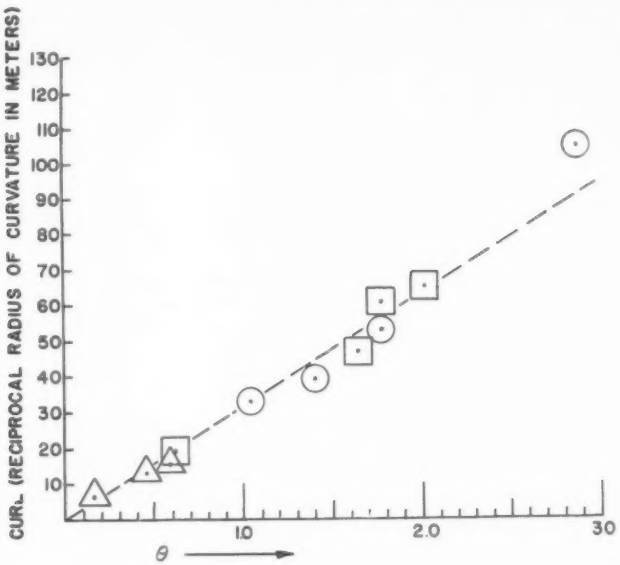

Fig. 4. Presentation of all curl data as one graph or function. Units used for calculation of θ values:

δ in mils, Δ in mils
RH_0 and RH in per cent
E = base modulus = 530,000 lbs/in.^{2}
E′ = gelatin modulus = 1.7×10^5 lbs/in.^{2} at 90% RH
5.7×10^5 lbs/in.^{2} at 50% RH
7.0×10^5 lbs/in.^{2} at 15% RH

⊙ VARIABLE BASE THICKNESS RH = 25 %
□ VARIABLE GELATIN THICKNESS RH = 28 %
△ VARIABLE GELATIN THICKNESS RH = 73 %

tively. It is worthy of note that the same shrinkage coefficient, β, appears in both the shrinkage and the curl equations. The average value of β from shrinkage measurements is 1.3×10^{-4}, as seen in the last column of Table I. The derivation of the equation for the film shrinkage coefficient is readily obtained by equating to zero the summation of all tensions in the film and by use of the usual stress-strain proportionality (see Appendix B).

Simplification of the Equations

Simplification can be achieved by expressing the equations for shrinkage and curl in terms of the dimensionless parameter, λ, which is simply the ratio of emulsion tensile strength ($E'\delta$) to support tensile strength ($E\Delta$).

From the equations of Fig. 5, it is seen that the shrinkage coefficient can be written:

$$\text{Shrinkage Coefficient} = \frac{2\lambda}{1+2\lambda}\beta + \beta_h. \qquad (1)$$

Likewise, the curl equation of Fig. 3 can be rearranged:

$$\text{Curl Coefficient}^* = \frac{6\lambda}{1+3\lambda}\beta. \qquad (2)$$

* By analogy with the shrinkage coefficient, the curl coefficient is defined as

$$\frac{\frac{\Delta}{r_2} - \frac{\Delta}{r_1}}{RH_1 - RH_2}.$$

In equation (2) for curl coefficient, it has been convenient to replace $1 + \frac{\delta}{\Delta}\left[4\frac{E'}{E} - 1\right]$ with $1 + 3\frac{E'}{E}\frac{\delta}{\Delta} = 1 + 3\lambda$. This is a very good approximation since the Young's moduli for the emulsion and the base are approximately equal and also because $\lambda \ll 1$.

Discussion

The equation relating film curl with the thicknesses and moduli of support and emulsion has been verified in Fig. 4, in which the experimental data fall on a straight line passing through the origin as predicted by the theory. Additional confirmation is obtained by comparison of the value of $\beta = 1.31 \times 10^{-4}$, obtained from the slope of the curl plot in Fig. 4, with the value of $\beta = 1.3 \times 10^{-4}$, calculated from the completely independent shrinkage data of Table I. The experimental data show an average deviation from the mean of about $\pm 18\%$, and thus the agreement between these independently determined values of β is better than one could expect and must be considered fortuitous.

The average value for β is 1.3×10^{-4}. Since β_h, the humidity expansion coefficient for "Cronar" polyester photographic film base, is 0.09×10^{-4}, the humidity coefficient of gelatin parallel to the base direction becomes 1.3×10^{-4} plus 0.09×10^{-4} and equals 1.4×10^{-4}. Measurements were made of the emulsion thickness at various relative humidities and the gelatin humidity expansion coefficient at right angles to the support was found to be appreciably larger, 37×10^{-4}.

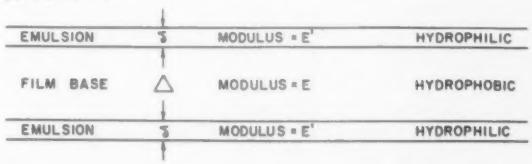

Fig. 5. Film under compressional stress resulting in shrinkage.

$$\text{Shrinkage coefficient} = \frac{\frac{L_0 - L}{L_0}}{RH_0 - RH} = \frac{2\frac{E'\delta}{E\Delta}\beta}{1 + 2\frac{E'\delta}{E\Delta}} + \beta_h$$

The emulsion coatings were generally made by normal "skim" coating of aqueous solutions containing roughly 5 per cent gelatin. In general, limed bone gelatin was employed in these films, and our experience indicates that other types, such as acid processed skin gelatin, behave quite similarly for curl and presumably also for shrinkage. Chrome alum or organic hardeners added in moderate amounts to the emulsion prior to coating did not alter curl greatly. In one experiment, the curl of rawstock film was compared with the same film after fixing in a standard acid-hardening fixing bath. The curl was essentially unchanged. However, when the sodium thiosulfate was replaced by sodium sulfate, and pH and hardener kept the same, curl was increased by roughly 15 per cent relative to the rawstock film. This latter experiment indicated that the potassium alum hardening contributed roughly 15 per cent to the curl, but that this was masked in the hardening fixer experiment by the removal of silver halides. The silver halide probably contributes to the curl by adding to the thickness of the emulsion layer. The silver halide grains dilute the gelatin but apparently behave like the "coarse aggregate" of the cement user by not appreciably lowering the Young's modulus. The density of silver bromide (6.5 gm/cc) is five times that of gelatin and thus contributes about 10 to 20 per cent to emulsion thickness. In these calculations, no attempt was made to correct for the presence of silver halide. The emulsion thickness was simply calculated from the known gelatin coating weight—ignoring, for the sake of simplicity, the contribution of silver halide to the total thickness.

In order to use equations (1) and (2), it is convenient to have a simple method for calculating the value for the parameter λ.

$$\lambda = \frac{E'\delta}{E\Delta}$$

Δ, the base or support thickness, is readily measured, and E, the base Young's Modulus, was 5.3×10^5 lb/in.[2] The Young's Modulus for gelatin, E', determined at three different relative humidities, showed considerable variation, especially at very high humidity, as shown by the data at the bottom of Fig. 4. The thickness of gelatin layers also varies with relative humidity: $\delta \equiv$ gelatin thickness in mils $= \frac{\text{Ctg. Wgt. (mg/dm}^2)}{324}$ [1 + 0.0037 RH]. However, within a reasonable range of RH, the product $E'\delta$ is relatively constant and equals $2 \times 10^3 \times$ (gelatin ctg. wgt. mg/dm^2). Thus $\lambda = \frac{2000}{E\Delta} \times$ (gelatin ctg. wgt. mg/dm^2). The gelatin coating weight which appears in the above equations is the coating weight of anhydrous gelatin. From the above equation for gelatin thickness, one can calculate the density of anhydrous gelatin by setting RH equal to zero. The result is a density of 1.3 gms/cc for anhydrous gelatin. This value for gelatin density is confirmed by the literature.[2]

It is expected that the density of gelatin will be relatively unaffected by changes in relative humidity in the normal range, because the volume and mass humidity coefficients are essentially equal for gelatin. By addition of the linear humidity coefficients in the three different directions, a value of 0.0040 is obtained for the volume humidity coefficient, i.e., $V = V_0$ [1 + 0.0040 RH]. Analysis of the literature[3] has yielded the mass humidity coefficient of 0.0047, i.e., $M = M_0$ [1 + 0.0047 RH], roughly.

Corroboration of the analytical operations used in obtaining the equation for curl would be reassuring, particularly since the derivation (Appendix A) is not a simple one. It has been found that the laminate structure of these films is exactly analogous to bimetal thermostat elements, and an examination of the appropriate references[4,5] has provided complete corroboration for the curl equation (7) in Appendix A. The equation of Timoshenko appears to be more general in that no limitation is placed on the relative thicknesses of the two laminated materials. In this derivation, the assumption is made that the emulsion layer is appreciably thinner $\left(\frac{\delta}{\Delta} = 0.2 \text{ or less}\right)$ than the support; and it is found that the equation of Timoshenko becomes identical with equation (7) when the former is expanded into a power series in $\frac{\delta}{\Delta}$, and terms in $\left(\frac{\delta}{\Delta}\right)^2$ and higher are dropped.

APPENDIX A — Theory and Calculation of Curl

In treating the base as a bending beam, the important variables are:

- r = radius of curvature of the curled film
- Δ = base thickness
- E = base flexure modulus (or Young's Modulus)
- δ = emulsion thickness
- E' = emulsion flexure modulus (or Young's Modulus) at the given relative humidity
- RH = relative humidity
- RH_0 = relative humidity at which r equals infinity (In this paper it is assumed that $RH_0 = 100$.)
- β = relative humidity shrinkage coefficient of emulsion parallel to the base less the same coefficient for the support.

Following the usual calculation methods,[6] we obtain a correlation of curl with the variable θ.

Referring to Fig. 3, from simple geometry,

$$\frac{L_0}{L} = \frac{r}{r - A}, \text{ or } \frac{1}{A} \times \frac{L_0 - L}{L_0} = \frac{1}{r} \equiv \text{curl}.$$

It is now assumed that the change in emulsion length with change in relative humidity and with change in stress follows the usual linear expansion law:

$$L = L_0\left[1 + \frac{S_g}{E'}\right][1 - \beta(RH_0 - RH)]. \quad (3)$$

S_g is the longitudinal stress produced in the gelatin by the resistance of the base to bending.

By rearrangement of equation (3)

$$\frac{L_0 - L}{L_0} = -\text{(emulsion strain)} = 1 + \left[1 + \frac{S_g}{E'}\right][\beta(RH_0 - RH) - 1].$$

Thus $\frac{1}{r} =$

$$\frac{1}{a + \delta/2}\left\{\beta(RH_0 - RH) - \frac{S_g}{E'}[1 - \beta(RH_0 - RH)]\right\}. \quad (4)$$

In the above equation there are two unknowns, viz., a, the position of the neutral axis, and S_g, the longitudinal stress in the emulsion. To calculate these quantities we make use of the equilibrium conditions that the summation of all longitudinal forces (tensions) is equal to zero and the summation of bending moments about the neutral plane is also equal to zero (W is sample width):

$$\text{Summation of tensions} = 0 = \frac{EW}{r}\int_{-a}^{\Delta - a} y\,dy + S_g W\delta.$$

$$\text{Summation of moments} = 0 = \frac{EW}{r}\int_{-a}^{\Delta - a} y^2 dy - S_g W\delta\left(a + \frac{\delta}{2}\right).$$

Integration of these two equations and suitable elimination yields:

$$a = \frac{\Delta}{2}\left[1 + \frac{1}{3\left(1 + \frac{\delta}{\Delta}\right)}\right] \quad (5)$$

$$S_g = \frac{E\Delta^2}{6\delta r\left(1 + \frac{\delta}{\Delta}\right)}. \quad (6)$$

Substituting (5) and (6) into equation (4), dropping squared and higher terms in $\frac{\delta}{\Delta}$, and assuming $\beta(RH_0 - RH)$ is much less than unity:

$$\text{Curl} \equiv \frac{1}{r} = \frac{6\frac{E'}{E}\frac{\delta}{\Delta^2}\beta(RH_0 - RH)}{1 + \frac{\delta}{\Delta}\left(4\frac{E'}{E} - 1\right)}. \quad (7)$$

It is of interest to note that when emulsion coatings of different thicknesses are on opposite sides of the base, the curl is calculated to a first approximation by using the thickness difference for δ in equation (7).

APPENDIX B — Theory and Calculation of Shrinkage

In the laminate of Fig. 5, the emulsion and the base lengths are constrained to be equal, i.e., $L = \mathfrak{L}$:

$$L = L_0\left[1 + \frac{S_g}{E'}\right][1 - \beta_g(RH_0 - RH)], \quad (8)$$

$$\mathfrak{L} = \mathfrak{L}_0\left[1 + \frac{S_b}{E}\right][1 - \beta_b(RH_0 - RH], \quad (9)$$

where S_g, S_b and β_g, β_b are the longitudinal stresses and humidity coefficients for the emulsion and the base, respectively. Furthermore, the sum of the forces in the lengthwise direction must be zero at equilibrium:

$$2S_g\delta - S_b\Delta = 0. \quad (10)$$

Equating (8) and (9) and using (10), yields

$$\frac{S_g}{E'} = \frac{\beta(RH_0 - RH)}{1 + 2\lambda}. \quad (11)$$

This value of S_g/E' when substituted in (8) yields

$$\frac{\frac{L_0 - L}{L_0}}{RH_0 - RH} = \frac{2\lambda}{1 + 2\lambda}\beta + \beta_b. \quad (12)$$

Acknowledgment

Acknowledgment is made to W. R. Holm and H. E. Behrens, J. M. Centa and R. B. Cook, W. W. Evans, and J. D. Overman for contributing data used in these calculations. R. B. Heiart and E. F. Haugh checked the derivations of the shrinkage and curl equations, respectively. Appreciation is expressed for the advice and cooperation of A. B. Jennings, D. R. White, and E. Meschter.

References

1. Dietz, A. G., *Engineering Laminates*. Wiley & Sons, New York (1949), p. 354.
2. Lange, N. A., *Handbook of Chemistry*, 7th ed. Handbook Publishers, Inc., p. 1384.
3. Mees, C. E. K., *The Theory of the Photographic Process*. The Macmillan Co., New York (1954), p. 70.
4. Dietz, *op. cit.*, p. 354.
5. Timoshenko, S., *J. Opt. Soc. Am.*, Vol. 11, p. 233 (1925).
6. Joos, G., *Theoretical Physics*. Blackie and Son, London and Glasgow (1940) p. 166.

PHOTOGRAPHIC SCIENCE AND ENGINEERING
Volume 1, Number 2, October 1957

A Color Chart for Use in Evaluating Quality of Color Reproduction

EDWIN J. BRENEMAN, *Research Laboratories, Eastman Kodak Company, Rochester, N.Y.*

To facilitate quantitative evaluation of the quality of color reproduction obtained with various photographic processes under given conditions of illumination, a color chart has been constructed. The twenty-four color patches include nine saturated colors, seven achromatic colors, and eight desaturated colors, among which are the familiar colors of flesh, foliage, and blue sky. The patches that represent the colors of natural objects have been matched to them as well as possible in spectral reflectance. Permanent pigments have been used so that the chart can be used repeatedly in direct sunlight without danger of fading or discoloring. The patches have uniform glossy surfaces so that unwanted surface reflections can be eliminated.

An analysis of the quality of a photographic color reproduction may be performed by determining, for a standard set of viewing conditions, errors in the reproduction of the hue, saturation, and brightness of various scene elements, and deducing from these errors and their interactions the effectiveness of the reproduction in representing the original scene. If this is to be done quantitatively, it is necessary that the colorimetric specifications of a variety of the elements in the scene be known. To facilitate the establishment and use of a mathematical expression for evaluating, in terms of colorimetric errors, the quality of color reproduction obtained with various photographic processes under given conditions of illumination, it is also necessary that the same scene elements be photographed in a specified manner whenever this expression is to be employed. These conditions are most easily met by the use of a color chart of known characteristics.

Design of the Color Chart

Such a chart should satisfy the following requirements:

1. Colors of low saturation should be included as well as highly saturated colors and achromatic colors. Among these should be the familiar colors of flesh, foliage, and blue sky.
2. The chart should be so designed that surface reflections, which modify colors, can be eliminated.
3. The colors should be resistant to fading by light, since the chart must often be used in direct sunlight.
4. The physical dimensions of the chart should be such that it may be handled easily and such that the reproductions of individual patches may be of sufficient size to permit measurements to be made with a densitometer or spectrophotometer.

Requirements (1) and (4) are easily satisfied in designing the chart. Details regarding these two requirements are discussed later in this paper. Requirement (2) implies that the patches should have an untextured surface of high gloss, since only for such a surface can surface reflections be controlled. Matte surfaces have the appearance of greater uniformity owing to the fact that, at the surface, light is reflected almost uniformly in all directions; therefore, it is impossible to eliminate these reflections by proper orientation of the object. With glossy samples, on the other hand, surface reflections are easily seen and can be eliminated by proper orientation (i.e., by reflecting a dark object in the surface as viewed from

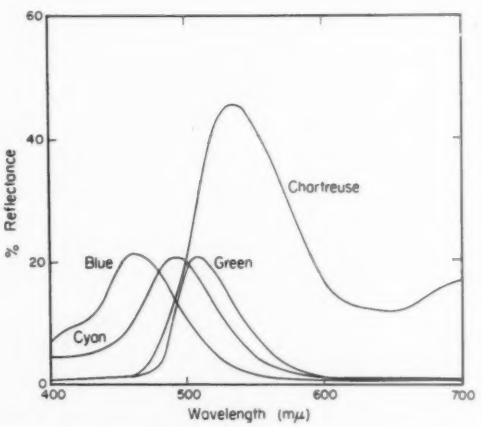

Fig. 1. Spectral reflectance (diffuse) of four saturated colors of the color chart.

Communication No. 1906 from the Kodak Research Laboratories. Received 6 June 1957.

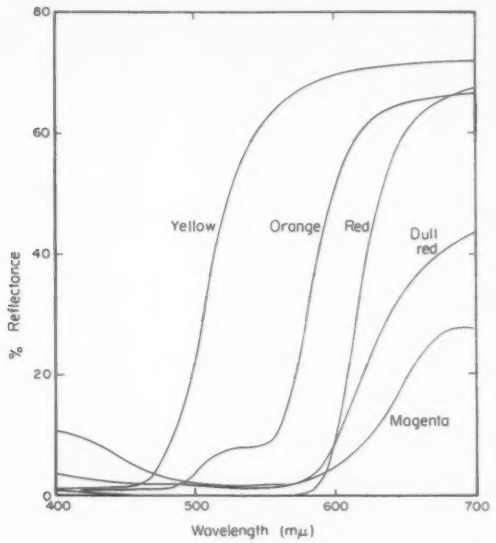

Fig. 2. Spectral reflectance (diffuse) of five saturated colors of the color chart.

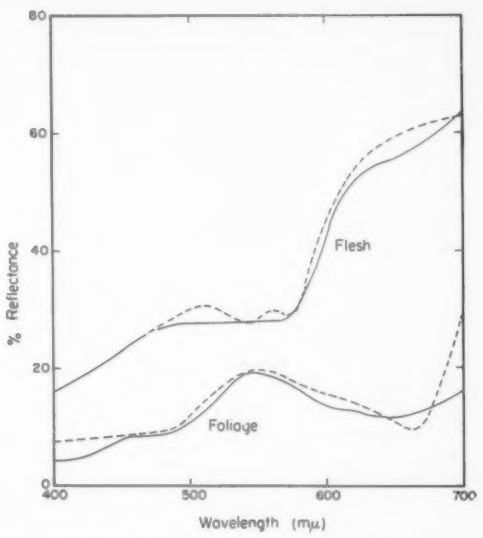

Fig. 3. Spectral reflectance (diffuse) of patches simulating the colors of flesh and foliage. Dashed lines indicate spectral reflectance of typical samples of Caucasian flesh and of foliage.

TABLE I

Composition and Colorimetric Specifications of Color-Chart Patches

(Different manufacturers' samples of a given pigment may have slightly different characteristics; however, in most cases the differences are slight and the different brands may be used interchangeably.)

Color	Pigments	C.I.E. Standard Source "C"		
		x	y	R (%)
Blue	Phthalocyanine blue and zinc oxide	0.150	0.123	3.3
Cyan	Phthalocyanine green, phthalocyanine blue, and zinc oxide	0.155	0.286	6.1
Green	Phthalocyanine green and cadmium yellow	0.195	0.570	7.6
Chartreuse	Cadmium yellow and viridian	0.346	0.564	30.1
Yellow	Cadmium yellow	0.464	0.492	56.8
Orange	Cadmium orange	0.580	0.392	21.5
Red	Alizarin glaze on titanium white	0.691	0.299	5.7
Dull red	Alizarin, cadmium yellow, and zinc oxide	0.548	0.300	5.5
Magenta	Cobalt violet, alizarin, and zinc oxide	0.379	0.208	3.3
Flesh	Cadmium red, strontium yellow, ultramarine blue, and titanium white	0.374	0.338	32.2
Foliage	Manganese blue, cerulean blue, yellow ochre, and titanium white	0.347	0.410	15.7
Sky blue	Antwerp blue, alizarin, and zinc oxide	0.236	0.250	23.1
Morning glory	Cobalt blue, cobalt violet, strontium yellow, and titanium white	0.239	0.226	10.8
Sand	Burnt umber, yellow ochre, chromium oxide, and zinc oxide	0.363	0.373	30.0
White	Titanium white	0.313	0.322	77.9
Neutral II	Zinc oxide, ivory black, and yellow ochre	0.305	0.316	26.6
Neutral III	Zinc oxide, ivory black, and yellow ochre	0.311	0.324	14.7
Neutral IV	Zinc oxide, ivory black, and yellow ochre	0.307	0.321	6.4
Neutral V	Zinc oxide, ivory black, and yellow ochre	0.307	0.322	2.2
Black	Ivory black	—	—	0.22
Ultraviolet reflecting gray	Flashed photographic paper	0.314	0.321	16.5
Brown	Burnt umber, burnt sienna, yellow ochre, and zinc oxide	0.405	0.358	2.7
Light green	Phthalocyanine green, cadmium yellow, and zinc oxide	0.246	0.396	31.9
Peach	Cadmium red, cadmium yellow, and zinc oxide	0.486	0.359	17.9

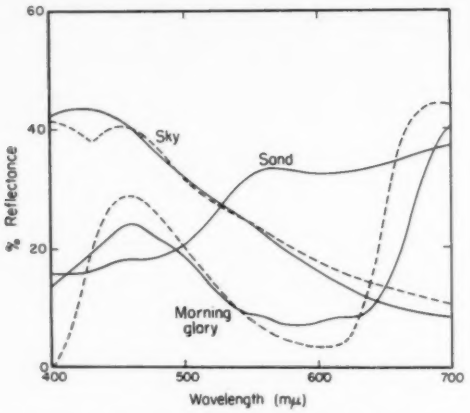

Fig. 4. Spectral reflectance (diffuse) of patches simulating the colors of blue sky, sand, and heavenly blue morning glories. Dashed lines indicate spectral reflectance of a typical morning glory and the energy distribution of zenith skylight. No curve for sand is included because of the wide variety of sand colors.

the camera position). It is because of this that colors of the highest saturation can be obtained only with glossy samples.

Requirement (3) suggests the use of permanent pigments (most of which are stable inorganic compounds) rather than dyes in making the patches. A wide variety of such pigments are available as artists' oil colors. In this form they are ground in just enough linseed oil to form a paste of butterlike consistency. They may be used in this form without the addition of more oil or reducer, thus providing very bright colors with the least tendency to yellow as the oil yellows with age.

A color chart has been made using such pigments. The necessary untextured glossy surface has been obtained by using for each patch a piece of cover glass to one side of which the artists' oils have been applied. The surface which is photographed is the inner glass-paint surface which is completely protected from abrasion and from atmospheric gases which may cause changes in the pigment or in the oxidized oil at the exposed surface of the paint film.

The chart consists of twenty-four patches, each 4 inches square. They are held in a wooden frame in four rows of six patches each. Such an arrangement

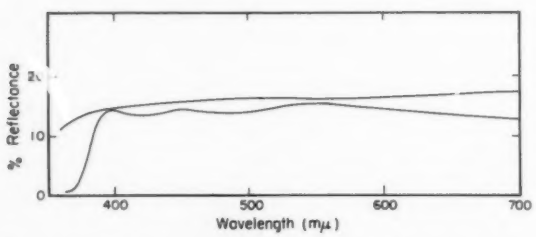

Fig. 5. Spectral reflectance (diffuse) of ultraviolet-reflecting gray (top curve) and a gray of similar density made with artists' oils (bottom curve).

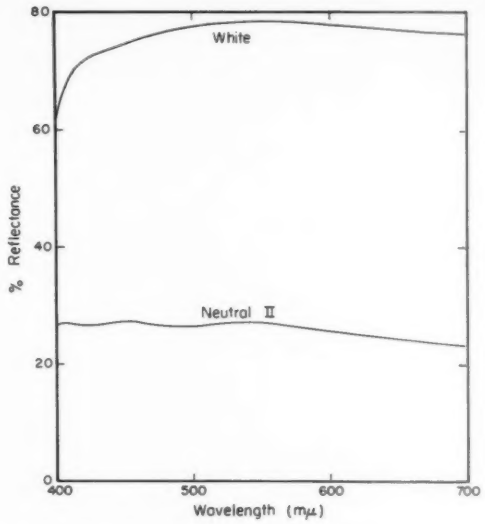

Fig. 6. Spectral reflectance (diffuse) of two of the achromatic color series of color-chart patches.

provides a chart of approximately the same proportions as the standard 35-mm color transparency, thus permitting the chart to be photographed with little wasted space in the transparency.

Nine of the twenty-four patches are colors of high saturation: blue, cyan, green, chartreuse, yellow, orange, red, dull red, and magenta. In making such patches, the "glazing" technique sometimes used by artists is helpful in producing greater saturation for a given brightness. This involves covering a white base with a transparent coat of the desired color. This technique is difficult to apply where large uniform areas are desired, since the resulting color is critically dependent upon the thickness of the transparent coating.* Of the colors mentioned, only the red patch was made in this way. The spectral reflectances (diffuse) of the patches are shown in Figs. 1 and 2.

Perhaps the most important colors in evaluating the quality of color reproduction are the familiar colors of flesh, foliage, and blue sky. These have been included in the chart, along with two others, sand and "morning-glory blue." Morning-glory blue, while not commonly occurring in color pictures, is included because it is seldom correctly reproduced by color films. Blue morning glories have a high reflectance in the far-red region of the spectrum where the sensitivity of the eye is low, but where most color films have high sensitivity. Therefore, the flower "appears" redder to the film than it does to the eye.

Because of the difference in spectral sensitivity of color films and the human eye, patches representing all the familiar colors mentioned must not only *appear*

*Stand oil, a polymerized linseed oil with excellent leveling ability and nonyellowing properties, is a very useful medium for such coatings.

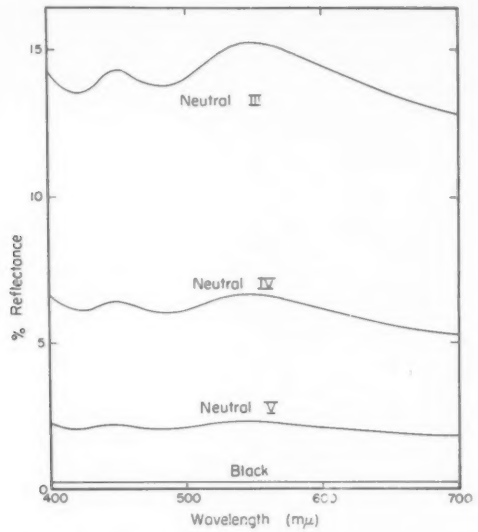

Fig. 7. Spectral reflectance (diffuse) of four of the achromatic color series of color-chart patches.

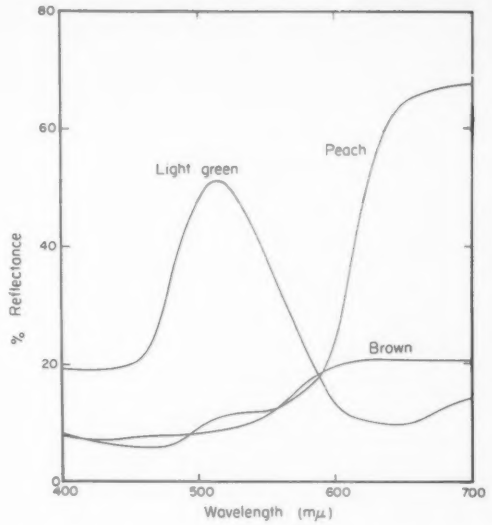

Fig. 8. Spectral reflectance (diffuse) of three desaturated colors of the color chart.

to be the correct color, but must have about the *same spectral reflectances* as the corresponding real objects. Only if this condition is fulfilled can reproductions of these patches be expected to indicate how the corresponding real objects will be reproduced. Since the results of mixing various pigments are hard to predict, the desired spectral reflectance for each of these patches was obtained only after many trials. Some of those trials were required merely to find the best pigments. Additional trials were needed to determine the proper proportions of each one. In Figs. 3 and 4, the spectral reflectance of each of the patches is given, along with the spectral reflectance of a typical sample of the corresponding natural object[1–4] (except in the case of sand, where it was felt the match need not be critical).

Seven achromatic colors have been included in the chart. They include a six-step series from white to black, made with artists' oils, and one additional gray which has the property of reflecting uniformly into the near-ultraviolet, as well as in the visible region of the spectrum. This patch was made by flashing a piece of Kodak Royal Bromide F-1 Paper which, after development in Kodak Dektol Developer as recommended and fixation in a nonhardening fixer, was joined with a gelatin-coated glass plate to form the glass color patch. The translucent photographic paper was then backed with a coating of patching plaster which has a high reflectance in the ultraviolet. The difference in ultraviolet reflectance between this patch and the other gray which most nearly resembles it in lightness is shown in Fig. 5. This difference will not have a very significant effect on the quality of the reproduction with the use of the average color film. Some color films have a very high relative sensitivity in the ultraviolet, however, so the inclusion of a gray with these characteristics seemed desirable. It would be desirable to make all the achromatic colors with the proper ultraviolet reflectance, but it is very difficult to make such patches which are uniform in density over their entire area and neutral in color throughout the entire series of grays. The spectral

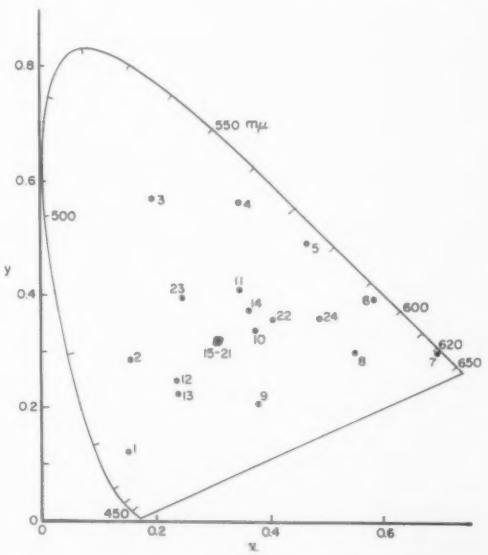

Fig. 9. Chromaticities of color-chart patches for C.I.E. Standard Source "C": 1, blue; 2, cyan; 3, green; 4, chartreuse; 5, yellow; 6, orange; 7, red; 8, dull red; 9, magenta; 10, flesh; 11, foliage; 12, sky blue; 13, morning glory; 14, sand; 15–21, achromatic colors; 22, brown; 23, light green; and 24, peach.

reflectance curves for the neutral patches are shown in Figs. 6 and 7.

Colors of low saturation are often very difficult to reproduce accurately, so several have been included in the chart. The familiar colors mentioned serve as part of this series. Others in the series are light green, peach, and brown. Spectral reflectances of these three patches are shown in Fig. 8.

The chromaticity and luminous reflectance of each of the patches are given in Table I. Also listed are the pigments which were used in mixing each color. The chromaticities are plotted in the C.I.E. chromaticity diagram in Fig. 9.

Use of the Color Chart

A chart of this type facilitates the quantitative evaluation of the quality of color reproduction. There are certain factors, however, which are not evaluated through the use of this chart. One of these is the effect of the ultraviolet sensitivity of a film upon the reproduction of distant objects. Also, specular reflections of skylight on glossy leaves or blades of grass modify the reproductions of these objects, depending on the ultraviolet sensitivity of the film.

In addition, there is the problem of the reproduction of metamers, or colors having the same appearance but different spectral reflectances. Metamers will not reproduce the same unless the spectral sensitivities of the color-film layers are linear combinations of the C.I.E. color-mixture functions. It is doubtful that any color film fulfills this condition. Therefore, it is not safe to assume that the reproduction of any given color indicates how colors which appear the same will reproduce. The best that can be hoped for is that each patch of the color chart has a spectral reflectance which represents approximately the average of such colors which, in practice, the film is called upon to reproduce. Since the factors mentioned are difficult or impossible to assess, it is desirable, when possible, to supplement the quantitative evaluation with reproductions of a variety of actual scenes.

When photographing the chart or supplementary scenes, it is important that a lens of about average spectral transmittance in both the ultraviolet and the visible regions of the spectrum be used. Also, in using the chart, it is important to avoid the illumination of the chart by light reflected from large colored objects nearby. As mentioned before, noticeable specular reflections from the surface of the chart should be eliminated. This may be accomplished by properly orienting one or two large black cards with respect to the camera and chart in such a manner that the reflections of the black cards cover the entire surface of the chart when viewed from the camera position. The energy reflected from these cards and, in turn, from the surface of the color patches will not be sufficient to contaminate the colors significantly.

References

1. Buck, G. B., and Froelich, H. C., *Illum. Eng.*, Vol. 42, p. 27 (1948).
2. Nickerson, D., Kelly, K. L., and Stultz, K. S., *J. Opt. Soc. Am.*, Vol. 35, p. 297 (1945).
3. Taylor, A. H., and Kerr, G. P., *J. Opt. Soc. Am.*, Vol. 31, p. 3 (1941).
4. "Filter Pack for Reproducing Unusual Flowers," *Kodak Color Notes*, No. 1, 1953, Eastman Kodak Co., Rochester, N.Y.

• Technicalia Photographica

FRANK SMITH

• Cameras, Components, and Accessories

Moving-Plate Camera for Nuclear Research

W. K. Dawson and B. W. Sargent, *Rev. Sci. Inst.*, Vol. 28, pp. 337–341 (May 1957).

A moving-plate camera, suitable for investigating the angular and energy distributions of photoprotons, is described. Two nuclear plates, 1 by 3 inches, coated with 200-micron emulsion, are accurately held with the emulsion surfaces vertical, parallel, and facing each other on a carriage. This carriage moves forward and backward in an evacuated tube at constant speed below the target and parallel to the x-ray beam. Targets are thin metal foils, 1.5 by 1 inches. The angles and energies of tracks recorded in each plate are 20 to 160 degrees and approximately 2 to 16 mev. The theory of the camera is developed in detail. Illustrated. 15 references.

360-Degree Azimuth Camera

A new 360-degree azimuth camera for recording horizon profiles and plane table work uses 35mm motion-picture film and is designed to assure accurate measurement of azimuth angles despite differential shrinkage of the recording film or photo prints. Film capacity is approximately 400 feet, and the camera is darkroom loaded but may be changed in daylight.

Current models of the camera may be obtained with a 12- or a 20-inch lens and with horizon scales of approximately 5 degrees or 10 degrees per inch. A flare-reducing mask permits photographing almost directly into the sun. The camera weighs about 20 pounds and mounts on a surveyor's standard tripod.

Aero Service Corp., 210 East Courtland St., Philadelphia 20, Pa., developed the camera.

The Miniature Camera Calibrator—Its Design, Development and Use

Harmon Q. Avera, *Photogrammetric Eng.*, Vol. 23, pp. 601–607 (June 1957).

The design of a calibrator for miniature cameras is outlined. The calibrator is fitted with an achromatic triplet lens as the collimator objective lens. The resolution target utilizes 14 elements to give resolution from 1 to 75 lines per mm for long focal length lenses and from 50 to 4,000 lines per mm for short ones. The major components of the structural framework and the control system are described in detail and a general approach to its use is outlined. Illustrated.

A Fast Auroral Camera

R. Montalbetti, *Canadian J. Phys.*, Vol. 35, pp. 280–283 (March 1957).

A motion picture camera is described which photographs auroral displays at one or more frames per second. The fast optical system and wide angle field of view are obtained with an $f/0.71$ objective and a spheroidal mirror. The camera has been found very useful in the study of auroral motions. Illustrated. 2 references.

Los Alamos 15-Million Frame/Second Camera

A new Model 8 camera has been developed by the staff of the University of California's Los Alamos Scientific Laboratory. It takes motion pictures of explosion and other high-speed phenomena at the rate of 15,000,000 frames per second for up to 96 consecutive pictures of a single event.

The original Model 6 camera, first announced in 1952, was capable of exposing at the rate of 3,500,000 frames per second. This was attained by the use of a two-sided mirror rotating at 10,000 revolutions per second, which swept the image-forming beam of light across a row of lenses to yield a series of photographs.

In the new Model 8 camera, a three-sided mirror revolves 23,000 times a second. The mirror is made of a special steel that has a tensile strength of over 300,000 pounds per square inch. It spins in a helium atmosphere on oil-pressure lubricated bearings, and is powered by a small helium-driven turbine.

Since an ordinary mechanical shutter cannot be used, an electric detonator is arranged to shatter a glass block in the light path, the shattered block being opaque enough to bar the light until a mechanical shutter can close.

The Model 8 camera is housed in a cast aluminum

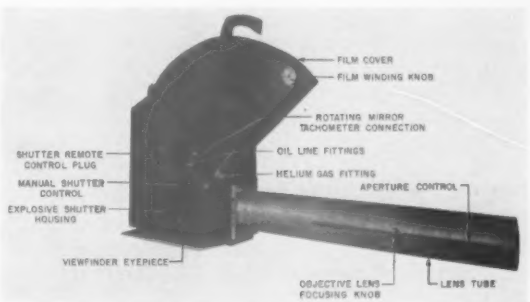

frame to withstand severe shocks, but is light enough to be carried easily, and simple enough to be operated by one man. Standard 35mm film in conventional cartridges is used.

New Polaroid 60-Second Camera

The new Model 150 Polaroid Land Camera produces finished post-card-size prints ($3^1/_4$ by $4^1/_4$ inches) in one minute, or positive black-and-white transparencies in two minutes, when Polaroid Land Projection Film is being used.

A coupled superimposed-image type rangefinder permits focusing from $3^1/_2$ feet to infinity. When the focusing knob is turned, the viewfinder is adjusted simultaneously to correct parallax and yield centered sharp images regardless of viewing angle or subject distance. A three-element, coated 135mm Cooke triplet lens is used and there is a single blade shutter with speeds to $^1/_{100}$ second. The shutter is synchronized for conventional and electronic flash exposures. The camera is manufactured by the Polaroid Corp., Cambridge 39, Mass.

New Bell & Howell Motion Picture Cameras

A spool-loading electric-eye 16mm motion picture camera has been developed by Bell & Howell Co., 8100 McCormick Road, Chicago 45, Ill. This camera joins the magazine-load model introduced last year.

The new Model 240EE camera embodies automatic exposure control, a 32-foot spring run, completely automatic threading, and other features of the standard 240 Series of Bell & Howell cameras, such as 100-foot film capacity, single frame, continuous-run lock, and a range of camera speeds from 8 to 48 frames per second. A B&H 20mm $f/1.9$ lens in focusing mount is supplied.

A new 8mm motion picture camera also provides automatic exposure control. In this camera, the photoelectric cell current is transmitted directly to a gear train that adjusts the diaphragm setting. The "electric eye" sets the diaphragm for proper exposure before the starting button is touched. It can operate the diaphragm through its full range of stops from $f/1.9$ to $f/16$ in less than one second. The camera can also be operated manually. Other features include a 10-foot spring run with continuous-run lock and single-frame exposure, a picture-window viewfinder which shows the subject in actual size and a B&H Super Comat 10 mm $f/1.9$ lens.

The schematic shows the 8mm electric eye camera. As light enters the recticular honeycomb lens combined with a baffle (A), its angular coverage is controlled to match the coverage of the camera lens. When the light reaches the photocell (B), it generates an electric current (the more intense the light, the stronger the current). As the electric current flows through the thermistor and resistor (C), it is compensated for temperature variations. At the meter coil (D), the current rotates or deflects the meter needle or needle pointer on the face of the camera. A gear

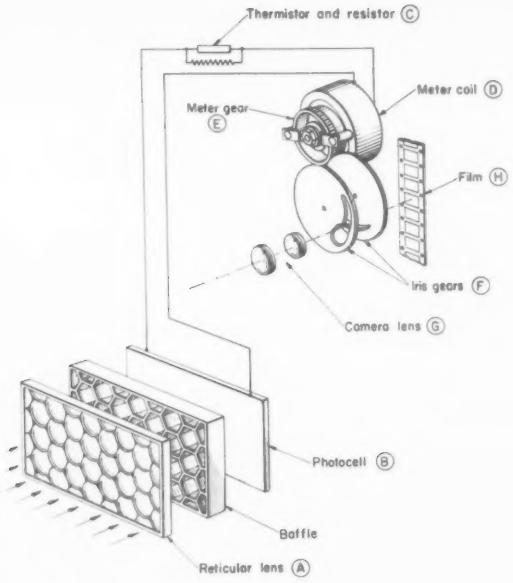

on the meter (E) engages the two iris gears or blades (F) which adjust the iris opening. The rotation of the meter opens or closes the iris to permit the correct amount of light to pass through the lens (G) to the film (H).

This action takes place in a fraction of a second. The inertia of the two iris gears is matched to that of the meter, to achieve stability of the iris even when the camera is moved during exposure. Otherwise, movement of the camera would cause the iris opening to drift across the lens or to change in size.

New Automatic Iris Control for Motion Picture Cameras

Mervin W. La Rue, Jr., *J. SMPTE*, Vol. 66, pp. 413–416 (July 1957).

The new Bell & Howell 200-EE camera incorporates a self-powered compact automatic iris control. Mechanical power to drive the lens iris originates from a small direct-current, permanent-magnet motor driven by mercury batteries. A photovoltaic cell deflects a relay according to average scene brightness, opening and closing the motor circuit to position the iris properly. The camera and its methods of use are described. Illustrated.

• Illumination

Safe Photoflash Unit Developed by U.S. Bureau of Mines

The Bureau of Mines, U.S. Department of the Interior, has developed a safe photoflash unit for underground use. The unit can be used anywhere in a coal mine without igniting coal dust or explosive gas. It consists of a $7^{7}/_{16}$-inch diameter reflector and socket and will accommodate photoflash lamps, up to and including the size 50 lamp, in an explosion-proof aluminum housing. The unit weighs 12 pounds and measures $8^{5}/_{8}$ inches in diameter and $5^{5}/_{8}$ inches in depth. The bulb can be safely inserted in the presence of explosive atmospheres.

Development of the safe photoflash unit followed that of an improved floodlight for use in motion picture photography of coal mining. Commercial firms are free to manufacture the photoflash and floodlight units without license.

Further details regarding both units may be obtained from the Branch of Electrical Mechanical Testing, Bureau of Mines, 4800 Forbes St., Pittsburgh 13, Pa.

Automatic Recarboning of Carbon-Arc Lamps

J. P. Latil, *J. SMPTE*, Vol. 66, pp. 338–340 (June 1957).

Methods are described for operating high-intensity carbon-arc lamps continuously for several hours. The great cost of the special carbons that are required as well as other factors limit their use, however. Less expensive methods would be of considerable utility and their development is encouraged. Illustrated. 4 references.

New High Intensity Rotating Positive Carbons for Motion-Picture Projection

R. B. Dull, J. G. Kemp, Jr., and E. A. Neel, Jr., *J. SMPTE*, Vol. 66, pp. 283–284 (May 1957).

New 10mm and 11mm high intensity projector carbons have been developed for rotating positive-carbon-type motion-picture projection lamps. These carbons, designed for 95-110 and 110-120 amperes respectively, give substantial increases in light and efficiency and operate with greater stability than former carbons of the same size and type. Performance data are presented. Illustrated. 1 reference.

Electroluminescense

Henry F. Ivey, *Sci. American*, Vol. 197, pp. 40–47 (August 1957).

When a luminescent substance such as zinc sulfide is placed in an alternating electric field, it emits light. This effect makes possible thin illuminating panels and many other useful devices. The effect and some of its applications are described. Illustrated.

• Instrumentation

Photographic Instrumentation at Ordnance Proving Grounds

Gerald Doughty, *J. Phot. Sci.*, Vol. 5, pp. 23–26 (March–April 1957).

A brief review of the camera instrumentation used at the U. S. Army Ordnance Proving Grounds. For

research and development work, the Ordnance Corps uses cameras of three basic types; the so-called high-speed motion picture cameras operating at speeds slightly above 100 frames per second (Mitchell), the acceleration camera (Bowen), and the very high-speed camera operating up to 15,000 frames per second (Fastax). All these types have been modified to serve particular requirements. The first two types are used principally on established ranges for recording the flight of missiles where data on space-time relationships are as a rule desired. The third type is used principally for close-up photography of mechanisms, events and missiles in flight (to record condition and orientation of the projectile), or a very high-speed sequence of events. Cameras of several other types are used for specialized ordnance work, where flexibility is sacrified to achieve quality in a particular field. Illustrated.

Optitherm Infrared Camera System

The Optitherm Infrared Imaging System consists essentially of a Barnes Optitherm Imaging Attachment mounted in front of a standard Barnes Radiometer, which converts infrared radiation into an electrical signal. A 10-degree field of view can be recorded on photographic film in as little as 30 seconds. Temperature differences of 0.2 C are easily detectable at maximum sensitivity.

In operation, a large plane mirror in front of the radiometer scans the field. The radiometer is stationary and "looks" into the scanning mirror so that the radiation enters it on axis at all times. A cam drive causes the mirror to oscillate horizontally to scan a line. At each extremity of the scan, the mirror is moved vertically by another cam through an angle equal to the height of the detector field of view. This continues until the radiometer has scanned a total view of 10 degrees by 10 degrees. A small mirror mounted on the back of the large scanning mirror deflects a spot of light emitted by an intensity modulated glow tube onto the photographic film. Since this mirror is rigidly fixed to the large scanning mirror, the light spot traces out a raster on the film which is the same as the radiometer scan pattern. The electrical output signal from the radiometer is used to modulate the light output of the glow tube, so that a "thermal" image of the scene is produced on the film.

The system is produced by the Barnes Engineering Co., 30 Commerce Road, Stamford, Conn.

Hycon Radar Strip Recorder

An airborne radar strip recorder has been developed by the Hycon Manufacturing Co., Pasadena, Calif. The recorder produces a photographic record of radarscope images on a slowly moving strip of $9\frac{1}{2}$-inch wide film. After exposure and rapid processing the film images are moved over a viewing screen. The 9- by 12-inch transparency is displayed 20 seconds after exposure and the speed of film travel controlled to correspond to airplane velocity. A permanent film record of the flight path of the airplane results, and the pilot, navigator, or observer has at his command a picture of the ground, day or night, in clear or cloudy weather. The strip recorder is adaptable to nearly all types of airborne radar and may be used on the ground to record radar or telemeter information relayed from airborne radar sets.

A monobath processing solution develops the exposed film at 130 F in 10 seconds. The fluid is applied to the film surface with a squeegee.

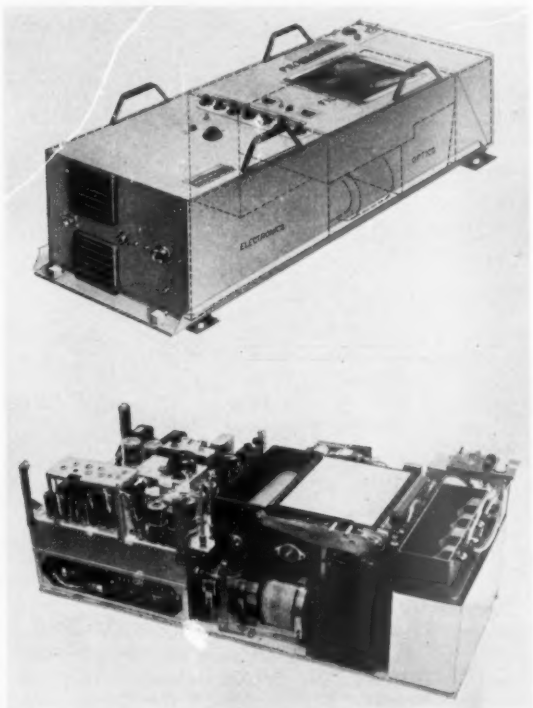

The Design of a 16mm Missile Camera

Robert B. Herden, *J. Phot. Sci.*, Vol. 5, pp. 20–23 (March–April 1957).

The design of a camera for installation in guided missiles is examined in terms of the general problem, the design objectives, the engineering approach, and the degree of success achieved. Illustrated. 2 references.

USAF Telescopic Photographic Recorder

The Telescopic Photographic Recorder, or TPR, is a mobile 6-ton unit used to photograph the flight of missiles, aircraft, and bombs. The unit can be operated remotely and is capable of photographing a 2- by 7-inch object at an altitude of 4 miles.

The instrument consists primarily of a 100-inch-focal-length reflecting telescope that measures 9 feet in length and 2 feet in diameter. It is equipped with a 70mm motion picture camera, two sighting telescopes, controls, and electronic and hydraulic components. The primary telescope is essentially a three-in-one system, since, by changing lenses in a transfer system, the effective focal length can be varied from 100 to 200 or 300 inches. A variety of color and neutral density filters are built in for use under different viewing conditions. The entire system is mounted on a modified four-wheeled 90mm gun mount which may be towed to location and stabilized by hydraulic jacks.

Signals from range radar as well as other information are fed into the system when a missile is fired and are utilized to orient the unit automatically in the direction of missile flight. When the missile is within range of the sighting telescopes, operators can take over and track it visually by means of an aided tracking system.

The instrument was designed and built by the Perkin-Elmer Corp., Norwalk, Conn., and will undergo range evaluation tests at the Air Force Armament Center at Eglin Air Force Base, Florida.

Millimicrosecond Photography With an Image Converter Camera

R. Carroll Maninger and R. W. Butenbach, *preprint of a paper presented at the 1957 IRE Convention, New York, N. Y., Precision Technology Inc., 66 South St., Livermore, Calif.*, 14 pp. (March 1957).

Photography of detonation propagation and the growth and decay of electrical discharges requires an ultra-high-speed camera. Such a camera and some unique problems associated with its development are described. The unit consists of a specially designed image converter tube, associated pulse circuitry, and oscilloscope recording camera. The tube acts both as a shutter and as the means for moving images across the face of the stationary recording film. It can take a multiple-frame sequence with controlled time spacing between frames and with exposure times during each frame as short as ten millimicroseconds. Illustrated. 13 references.

A Photographic Recording Microphotometer

J. Bor, *J. Sci. Instr.*, Vol. 34, pp. 140–141 (April 1957).

A simple method of converting a nonrecording microphotometer into a single-beam recording instrument of good discrimination and high speed is described. The instrument is capable of handling a wide range of photographic densities. Illustrated.

High-Speed Photography

J. S. Courtney-Pratt and D. P. C. Thackeray, *J. Phot. Sci.*, Vol. 5, pp. 32–42 (March-April 1957).

A number of devices and methods used in high-speed photography are described and discussed. The survey includes drum cameras, image dissection cameras, image converter tube photography, image splitting devices, and light sources. Illustrated.

• Optics

Anamorphic Lens System

Seymour Rosin, *J. SMPTE*, Vol. 66, pp. 407–409 (July 1957).

An anamorphic lens known as "Scanascope" has been developed for use in motion picture and television work. The optical design is described and performance data given. A unique coupling arrangement allows this lens to be used interchangeably with camera lenses of different focal length in a unit focus

arrangement. Application of this system to the Mitchell NC and BNC cameras is described. Illustrated.

Aberration Permissible in Optical Systems

H. H. Hopkins, *Proc. Phys. Soc., Sec. B.*, Vol. 70, Part 5, No. 449B, pp. 449–470 (1 May 1957).

A criterion for permissible lens aberration is proposed, i.e., the response of an optical system for a given spatial frequency shall not be less than 0.08 times the response of the same system in the absence of aberration. In this way the aberration tolerance is related to the number of lines that must be resolved with good contrast. The method is applied to defect of focus, spherical aberration, coma, and astigmatism. The best form of correction and focal plane is determined by the same method. The results are expressed by approximate formulas for the lower spatial frequencies which are those of importance in other than very highly corrected systems. Illustrated. 3 references.

Reticle-Projecting Microscope

W. C. Davis, *Rev. Sci. Instr.*, Vol. 28, pp. 577–579 (June 1957).

A brief description of a microscope modification which makes the microscope useful for examining the image-forming qualities of various optical systems. The modified microscope produces a test pattern for the optical system under test, and at the same time is used to examine the image of that pattern which the optical system forms. Illustrated. 1 reference.

An Optical Scanning and Recording System for a Photoelectric Optical Bench

T. N. J. Archard and D. H. Rumsey, *Electronic Eng.*, Vol. 29, pp. 231-233.

A method of lens assessment on an optical bench involves scanning a narrow slit of light passed by the lens under test, and measuring the light flux photoelectrically. A graph is then plotted from the results obtained. The apparatus described performs these functions automatically, using impulse motors, a direct-current amplifier and a recording milliammeter. Illustrated.

Fiber Optics — Part I

"Optical Properties of Certain Dielectric Cylinders."

N. S. Kapany, *J. Opt. Soc. Amer.*, Vol. 47, pp. 413–422 (May 1957).

Various novel applications of transparent fibers depend on their high light conductivity and appropriate radiation properties. Different factors affecting the optical properties of dielectric cylinders and methods of measuring them are discussed. The geometrical optical properties of cylindrical and conical channels are examined. A microinterferometric technique is described for the continuous testing of cylindricity and of the variation in diameter of long lengths of fibers. The surface structure of drawn glass fiber has been studied with the electron microscope and the absolute refractive index and inhomogeneities in fibers measured by means of multiple beam interference. The bi-refringence and light transmittance of various fibers has been measured and the optical properties of bent fibers have been studied. The modification of radiation patterns of fibers curved on circular arcs has been investigated also and photometric measurements made. Illustrated. 10 references.

Fiber Optics — Part II

"Image Transfer on Static and Dynamic Scanning with Fiber Bundles."

N. S. Kapany, J. A. Eyer, and R. E. Keim, *J. Opt. Soc. Amer.*, Vol. 47, pp. 423–427 (May 1957).

The image transfer through a stationary bundle of fibers can be thought of as a static sampling of the illuminance of the image at the entrance end of the bundle by each fiber element. This discrete sampling limits the band width of signals which can be transmitted and the end of the component fibers form an obtrusive pattern in the received image. The resolving power of the system, however, is improved materially by random dynamic scanning with the film bundle. Also, the individual fiber ends are thus blurred out and the obtrusive pattern formed by them is destroyed. Because each fiber integrates the flux falling upon its entrance aperture, the entire picture format scanned dynamically is reproduced at the frequency response characteristic of a uniform disk whose diameter is equal to that of the component fibers. An experimental setup for the detailed investigations of the effect of dynamic scanning with a fiber bundle is described. A gain of 100 per cent in resolution by this method is illustrated by photographs and by densitometer traces of various test objects which have been scanned both statically and dynamically. Illustrated. 3 references.

Fiber Optics — Part III

"Field Flatteners."

N. S. Kapany and R. E. Hopkins, *J. Opt. Soc. Amer.*, Vol. 47, (July 1957).

A method of field flattening using a bundle of transparent fibers is studied in some detail. Different optical arrangements of field flatteners are proposed and their relative merits are investigated. An improved type of field flattener which also acts in the same manner as two Fresnel lenses has been developed and the term "Fresnel-lens-type field flattener" is proposed to denote it. A gain in image quality and weight of a flight periscope system seems possible by the use of such a field flattener. The methods of alignment and fabrication of these field flatteners are described. Working models using 200-micron diameter glass fibers have been constructed which demonstrate the expected gain. Illustrated. 3 references.

• Projection

Hi-Speed Additive Color Compensating Head

The Fish-Schurman Hi-Speed Additive Color Compensating Head for continuous printing at 200 feet per minute is equipped with a single 1000-watt, high-efficiency light source. Three electromechanically operated light valves provide color changes in 5 milliseconds. Each light valve is controlled by five small solenoids to provide 32 printer steps. The light valve opening may be adjusted to compensate for color print material changes without altering the 32 step arrangement.

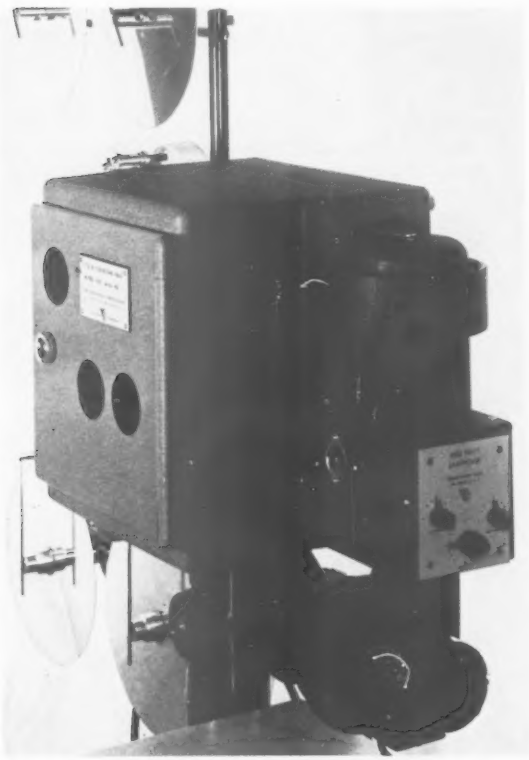

High light efficiency is obtained with the aid of interference multilayer all-dielectric beam splitters. Separation of the color bands is accomplished without overlap and with little light loss.

Originally designed to operate with the Bell & Howell Model E printer head, it is now available to fit the heads on Models D and J. The machine is manufactured by Fish-Schurman Corp., 70 Portman Road, New Rochelle, N.Y.

Transpaque II All-Purpose Still Picture Projector

The Transpaque II is claimed to be the first projector that uses a single projection head and lens for opaque, transparency, table, and rear projection. It is manufactured by Projection Optics Co., Rochester, N.Y.

The projector not only projects 10- by 10-inch transparencies or 11- by 11-inch opaques, but it can be moved and set directly on large objects, so that maps, drawing boards, display cases, or any areas measuring 11 by 11 inches can be projected.

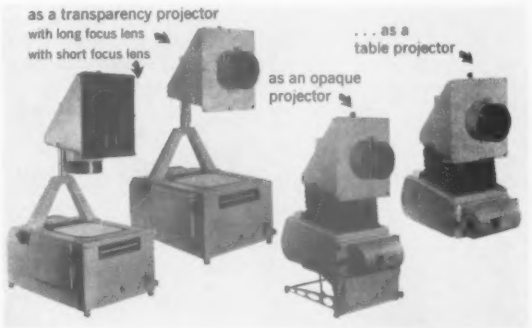

Lenses varying in focal length from 4 to 40 inches are available, enabling the operator to obtain the right size image for any screen at any distance.

The projector may be purchased for opaque, for transparency, for table, or for rear projection only, and the components for any of the other applications may be added later. The change from one kind of projection to another is said to be made quickly and easily.

New 2-by-2 Slide Projector for Television

A. E. Jackson, R. D. Houcks, and R. F. Roundy, *Broadcast News*, Vol. 94, pp. 64–73 (April 1957).

A new 2- by 2-inch slide projector has been designed especially for television broadcasting. The projector, designated Type TP-7A, is said to provide maximum operational convenience, high quality performance, and reliability. Illustrated.

A New High-Speed Spray Processor for 16/35mm Black-and-White Negative or Positive Film

Edward V. Lewis, *J. SMPTE*, Vol. 66, pp. 419–421 (July 1957).

The compact, high-speed processor employs modular "building-block" units that are spray chambers of uniform construction. The article describes a reliable method for providing a vaportight seal in a spray chamber and a washdown system that facilitates preventative maintenance. Illustrated.

• Techniques and Applications

U. S. Army Signal Corps Fast Facsimile

A new facsimile system has been developed by the U.S. Army Signal Engineering Laboratories. The

portable radio facsimile unit can deliver a high quality photographic reproduction 5 minutes after the original camera exposure has been made at another location.

The new facsimile equipment fits easily into the back of a radio-equipped jeep or car and can send a picture to its companion receiver 40 miles away. The set can also send its signals over standard telephone lines or by long-range radio circuits. The system combines high-speed Army picture-sending techniques with Polaroid film that produces a finished print one minute after exposure or receipt. No darkrooms are needed.

Reducing Trajectory Data With Oriented Cameras

Rodney P. Larson, *Industrial Laboratories*, Vol. 8, pp. 84–89 (August 1957).

A discussion of a method of reducing trajectory data by means of a theodolite-oriented Bowen Camera and a Tracking Bowen Camera. The method is used at Project SMART (Supersonic Military Air Research Track) at Hurricane Mesa in southern Utah. Illustrated.

LogEtronography

Elmer G. St. John, M.D., and Dwin R. Craig, *Amer. J. Roentgenol.*, Vol. 78, pp. 124–133 (July 1957).

LogEtronics is a method of photographic printing, and its application to roentgenography is described. It is claimed that LogEtronics simplifies the task of making high quality reproductions of roentgenograms for use in publications, teaching, and filing, and that it provides the radiologist with a new form of visual and diagnostic aid. Illustrated. 7 references.

A Color Schlieren System for High-Speed Photography

George E. Hays, *J. SMPTE*, Vol. 66, pp. 355–356 (June 1957).

A simple color schlieren system has been developed which uses the chromatic aberration of two spherically corrected field lenses to produce a color image. This system is used extensively in explosion studies and other investigations requiring high-speed photography. Illustrated. 4 references.

Photographic and Magnetic Sound Reproduction From One Track by Means of Infrared Light

George Lewin, Chief, Pictorial Engineering Office, Army Pictorial Center, has reported that magnetic sound tracks on motion-picture film, previously believed to be opaque, are reasonably transparent to infrared radiation. Therefore, it is possible to superimpose a magnetic stripe over a full-width photographic sound track and still obtain good quality sound reproduction. At the same time, the magnetic stripe may be used for an entirely independent recording. Maximum fidelity reproduction may be obtained from such a magnetic track at only slight loss of volume from the photographic track. The system should be immediately applicable to the JAN motion picture projector which employs a lead-sulfide photoconductive cell that is infrared sensitive, provided the projector is equipped with a magnetic sound reproducer. Additional tests will be necessary, however, to evaluate fully the commercial feasibility of the superposed sound track scheme.

An article by Mr. Lewin, describing his studies, appears in the *Journal of the SMPTE*, Vol. 66, No. 9, pp. 517–522 (September 1957).

The Myriatron

G. H. Lunn and R. A. Chippendale, *Electronic and Radio Engineer*, Vol. 34, New Series No. 5, pp. 156–160 (May 1957).

The Myriatron image dissector tube for high-speed cinematography is briefly described. The Myriatron tube combines the principles of image dissection with the image converter. It is similar to a conventional image converter except that the photocathode is active only in areas 0.001 inch square, spaced 0.01 inch on centers. The picture of an object seen on the fluorescent screen of the tube, therefore, is equivalent to that seen through an opaque screen pierced with a corresponding regular array of small square holes whose total area is only $^1/_{100}$th of the screen area. Consequently, the major, unused area of the screen is available for the display of other "pictures." Illustrated. 15 references.

A 16mm Television Recording Channel

M. E. Pemberton, *The Marconi Review:* Part I, Vol. 20, No. 124, pp. 4–22 (1st Quarter, 1957); Part II, Vol. 20, No. 125, pp. 39–50 (2nd Quarter, 1957).

The Marconi Television Recording Channel B.D. 679 has been developed to meet the growing demand for television recordings. The equipment is designed to operate at 625/405 lines 50 fields per second or 525 lines 60 fields per second.

The over-all channel and the recording monitor are described in Part I. Part II describes the fast pull-down camera and its driving unit, the flywheel synchronizing panel, and the power supplies. Illustrated. 3 references.

Electron-Image Recording by Xerography

P. B. Sewell, *Nature* (London), Vol. 179, pp. 773–774 (April 13, 1957).

A discussion of the application of xerography to the recording of electron images of the type produced in electron microscopes and electron diffraction cameras. Electron diffraction patterns have been recorded on specially prepared vitreous films of approximately 60 microns thickness, by use of an accelerating voltage of 50 kv. The selenium plates employed required an exposure similar to that used with Ilford N. 50 photo-

graphic emulsions. A diffraction pattern just visible on the fluorescent screen requires an exposure time of about 5 seconds. The following features of the xerographic technique are considered particularly noteworthy: (1) The vitreous selenium plates are free from outgassing effects at room temperature. (2) Xeroradiographic plates can be used for recording electron images produced in electron-optical instruments at beam-accelerating voltages between 45 and 55 kv. (3) Such plates require an exposure similar to that used with the high-contrast photographic materials commonly employed in electron microscopy and electron diffraction. (4) The utilization of suitable developing techniques makes possible better image resolution than attainable with conventional photographic materials and without sacrifice in plate sensitivity. (5) The high image-contrast and wide exposure latitude of xeroradiography are advantageous in the recording of electronmicroscope images which frequently are of low contrast. Illustrated. 6 references.

Atoms Visualized

Erwin W. Müller, *Sci. American*, Vol. 196, pp. 113–122 (June 1957).

The field ion microscope makes pictures of atoms in a metal crystal by accelerating positive ions from a fine needle of the metal to a fluorescent screen. Photographs of the fluorescent screen provide the visualization of the atoms.

Photographs of the atoms are made "in color" by a three-step technique. First, a photograph in black and white is made in green light of the image on the screen of the tip of the needle before any changes are made in its surface. Later, when changes have occurred in the positions of some atoms, a black-and-white photograph is made in red light. The green-light and red-light pictures are then superimposed and a color photograph made with a conventional camera. Whenever the positions of the atoms are unchanged, the atoms appear yellow—the sum of the green and the red. Where green dots appear, atoms were present in the first picture, but were removed before the second. Red dots, on the other hand, mark atoms recorded only in the second picture. Illustrated.

An Evaluation of the Application of Thulium-170 to Industrial Radiography

James W. Dutli and Dana E. Elliott, *Nondestructive Testing*, Vol. 15, pp. 112–114 (March-April 1957).

An Argonne National Laboratory Portable X-Ray Unit, utilizing the isotope thulium-170, has been evaluated for its applicability to industrial radiography. Radiographic techniques, resolution, and sensitivity data are presented for magnesium, aluminum, steel, and plastic materials. Experimental data on the radiation spectrum are also included. It is concluded that thulium-170 is suitable for radiography of very thin metal sections. The light weight and compactness of the unit should make it useful when space limitations or economy preclude the use of x-ray machines. Illustrated. 7 references.

High-Frequency Cinematography in the Shock Tube

H. Shardin, *J. Phot. Sci.*, Vol. 5, pp. 17–19 (March-April 1957).

The advantages of high-frequency cinematography were discussed in a previous paper, published under the same title in the proceedings of the Third International Congress on High-Speed Photography. The present article refers to additional results obtained from the experimental technique, and to further clarification of the phenomena associated with flow over a wedge in a shock tube. Illustrated. 4 references.

Detonation Studies of Pentolite Sticks

Morton Sultanoff, *J. Phot Sci.*, Vol. 5, pp. 27–31 (March-April 1957).

Recent developments in high-speed photographic instrumentation have made it possible to observe in greater detail the luminosity of exploding pentolite charges, and to associate this luminosity with physical detonation and shock phenomena. By studying and identifying the luminosity in separate phases and combining the results, an over-all model is obtained, which includes a "preliminary light," the detonation front, a "dark-space," and finally, luminous air shock. The results of these studies have also been used to explain and clarify questionable observations made by earlier techniques. Illustrated. 7 references.

A Photographic Personnel Dosimeter for X-Radiation in the Range From 30 Kev to Beyond 1 Mev

Margarete Ehrlich, *Radiology*, Vol. 68, pp. 549–554 (April 1957).

A photographic personnel dosimeter has been developed whose main feature is its usefulness over the photon energy range from about 30 kev to beyond 1 mev. It may be employed to interpret x-ray exposures from 250 milliroentgens to 3 roentgens with an accuracy of ±20 per cent, and exposures from 3 roentgens to 6 roentgens with an accuracy of ±30 per cent. No knowledge of photon energy is required. If the photon energy is known to be in the million-volt region, the range of the dosimeter can be extended to 600 roentgens. Illustrated. 7 references.

The Use and Limitations of Flexible Fluorescent Intensifying Screens in Ship Radiography

K. G. Roberts, *Nondestructive Testing*, Vol. 15, pp. 162–165 (May-June 1957).

The technique of relating tube kilovoltage in radiography to material density and thickness has been used successfully in high quality radiography of equivalent steel thickness of $1\frac{1}{2}$ inches and less, with

260-kv x-ray equipment and lead intensifying screens.

Consideration is given to the increased intensification from fluorescent screens to determine whether greater thicknesses may be radiographed, under the same conditions of exposure time and source-to-film distance, without undue loss of sensitivity. By employing flexible fluorescent intensifying screens, it is shown that up to $2^1/_2$ inches of steel can be radiographed with 260-kv x-rays, in a standard exposure time of 4 minutes, at a source-to-film distance of 30 inches. The radiographic sensitivity is slightly over 1.5 per cent, but it can be improved to less than 1.5 per cent by replacing the fluorescent front screen with a 0.005-inch lead screen and consequently limiting the maximum steel thickness to $2^1/_4$ inches.

In radiography with cobalt-60, there is very little time advantage with fluorescent screens and the resultant sensitivity values are about 2 per cent or greater. The combination of no-screen film and lead intensifying screens yields a sensitivity of 1.5 per cent in moderate exposure times and appears to give the optimum results for high quality radiography. Illustrated. 5 references.

Xeroradiography

D. B. Slauson, *IRE Transactions on Medical Electronics*, PGME-8, pp. 1–5 (1957).

A brief review of the properties of the xeroradiographic plate and its development, viewing, plate speed, and application.

The Trend of Facsimile in Military Communications

A. G. Cooley, *Signal*, Vol. 11, p. 42, 44, 46 (July 1957).

A brief technical review of facsimile since its inception in 1848, with particular emphasis on its military applications. Illustrated.

The Use of Multiple-Film Techniques to Speed Industrial Radiographic Inspection

Ralph E. Turner, *Nondestructive Testing*, Vol. 15, pp. 146–150 (May-June 1957).

In the examination of multithickness specimens, the radiographer is often faced with two choices: he may make two or more exposures, each geared to a definite thickness range; or he may make a single exposure using two or more films of different radiographic speeds, the slower film to record the thin sections, the faster film or films to record the thick sections. The latter method makes unnecessary the setting up of more than one exposure and thus speeds examination considerably. The range of thickness recorded on the film, however, is limited by the various radiographic speeds of the films used at the selected exposure value. Illustrated.

• Miscellaneous

Sylvania Image-Producing Panels

A new image-producing panel called "Sylvatron" utilizes the principles of electroluminescence and photoconductance. It is manufactured by Sylvania Electric Products, Inc., 1740 Broadway, New York 19, N.Y.

"Sylvatrons" consist of flat electroluminescent glass panels coated with thin photoconductive and electroconductive control layers. When electrical or optical signals and a power source are applied to the panels, a visual display or image is produced. The panels perform the functions of visual image production, light storage, and image conversion.

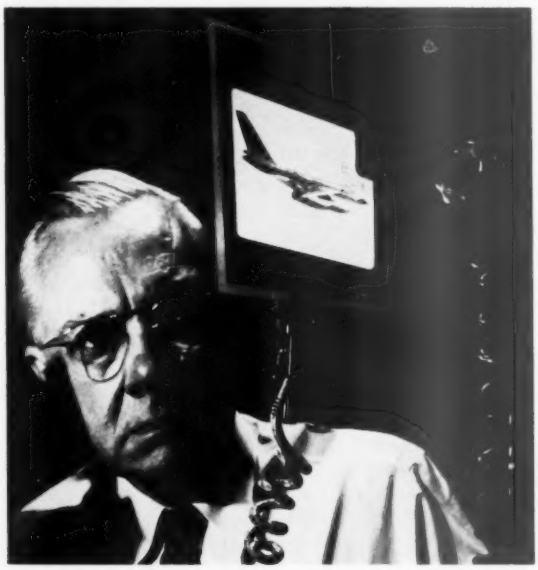

At present three basic types are completed but many other combinations are under development. The three basic types are: (1) An electroluminescent panel on which the position of a mobile dot of light can be manipulated electrically. (2) A display panel which reproduces optically the track of a mobile spot of light. The image thus created can then be held or "stored" indefinitely in visible form on the panel. (3) An electroluminescent panel which can reproduce optically a motion picture with good resolution and rapid response.

Combinations of these three types lend themselves to certain applications. The combination of Types 1 and 3 can be used to reproduce motion pictures electronically. The panels have been produced in the laboratory in 2-inch and 4-inch squares, and larger sizes are under development.

Photoprogress

Frank Smith, *Signal*, Vol. 11, pp. 36–38, 40 (July 1957).

A bi-monthly progress report of new and significant developments in the field of photographic science and engineering. This paper briefly describes and discusses: Photography of Atoms; the U.S. Air Force's new "Cat Eye" Light Amplifier; Electron-Image Recording by Xerography; Image Converters in Photography; Exicon-Expanded Image Contrastor; Fisheye 180-Degree Camera; and Viewing Negatives as Positives. Illustrated.

The Nimythoscope

Hugh T. O'Neill and William J. Nagel, *Photogrammetric Eng.*, Vol. 23, pp. 533–535 (June 1957).

A brief description and discussion covering an instrument for viewing any type of photography in gradually decreasing size (or scale) for many purposes. Illustrated.

"Exicon"—Expanded Image Contrastor

The "Exicon" (expanded image contrastor) x-ray viewer is designed to perform three different functions in order to extract a maximum amount of information from a radiographic image. It is said to enhance x-ray contrast in "gray scale" variations, increase readability by utilizing full color, and magnify the area being viewed.

The unit consists essentially of monochrome and color monitors, an operator's console, and a flying spot scanner. A radiograph placed before the flying spot scanner is magnified and separately reproduced in enhanced monochrome and color. It may be shifted about to obtain magnified images of any portion. The system may be used in conjunction with closed circuit color TV installations.

The "Exicon" is produced by Philco Corp., G&I Div., 4700 Wissahickon Ave., Philadelphia 44, Pa.

Principles of the Light Amplifier and Allied Devices

T. B. Tomlinson, *J. Brit. Inst.*, Vol. 17, pp. 141–154 (March 1957).

The necessary component parts of a light-amplifying system are enumerated and the advantages of solid state devices noted. A system is outlined which consists of a photoconducting layer in series with an electroluminescent phosphor layer. Various practical constructions are described and attention drawn to the difficulties of manufacturing a picture-reproducing device of large areas. Optical feedback depends on the spectral emission distribution of the electroluminescent layer and the spectral response of the photoconductor. An amplifier with optical feedback such that the loop gain exceeds unity can be triggered by a light pulse and then remain in the light-emitting condition until the supply voltage is reduced. The author describes such an electrooptical binary switch using ZnS and CdS powder layers or single crystals. Complex combinations of such units could be employed in shift registers, scaling circuits, etc., and novel circuits are suggested which employ light as the means of triggering and coupling. These devices would be of miniature size and would need few, if any, associated conventional components. Limitations of switching time and possible future developments are also discussed. Illustrated. 9 references.

The Nature of Photographic Sensitivity

J. W. Mitchell and H. H. Wills, *J. Phot. Sci.*, Vol. 5, pp. 49–70 (May-June 1957).

A review of the work on photographic sensitivity which has been carried out by the author and his colleagues and of the conclusions that have been drawn from it. The earlier concept of the sensitivity speck has been replaced by that of the sensitivity center. The sensitivity speck was assumed to consist of silver or of silver sulfide and to have the function of concentrating silver atoms; the sensitivity center is a region of enhanced reactivity associated with a crystal imperfection. It is postulated that the principal function of the silver sulfide is to trap positive holes and thus to prevent the regression of latent image specks. According to present ideas, the latent image is formed in two stages. In the primary stage, electrons and positive holes are liberated, the positive holes are trapped and interstitial silver ions are formed. In the secondary stage, the silver ions combine with the conduction electrons to form, first latent preimage specks, then latent sub-image specks, and finally stable latent image specks. Reciprocity failure is discussed. The new approach to the theory of photographic sensitivity, in which the role of kink sites is emphasized throughout, leads to the enunciation of four basic principles which must be satisfied by any theory of the formation of the latent image. Of these, only the Gurney-Mott principle has previously been recognized. Illustrated. 81 references.

Some Practical Considerations in the Analysis of High-Speed Motion-Picture Data

William G. Hyzer, *J. SMPTE*, Vol. 66, pp. 357–360 (June 1957).

The usefulness of motion-picture images for both visual and quantitative analysis depends on several factors, including optical resolution, image blur, image contrast, image-shape characteristics, and differential movement of the image from frame to frame. These factors were evaluated in a series of practical tests, using standard analytical techniques and equipment, to determine their effects on the overall performance of 16mm film. Illustrated. 2 references.

A Century of Progress in the Synthesis of Dyes for Photography

L. G. S. Brooker and P. W. Vittum, *J. Phot. Sci.*, Vol. 5, pp. 71–88 (May-June 1957).

Dyes had no place in the daguerreotype and other photographic processes in vogue a century ago. Today, dyes are vital not only to color photography but also in much of black-and-white photography. They are used as color sensitizers, as desensitizers, for the prevention of halation effects, and in filter layers. The development of these applications of dyes is reviewed. Illustrated.

Strato-Lab Balloon Photography

Eugene P. Griffin, *Photogrammetric Eng.*, Vol. 23, pp. 582–587 (June 1957).

A narrative account of the first attempt to obtain and utilize aerial photographs taken from a free-flight, unmanned plastic balloon that carried a mapping camera in a pressurized gondola to an altitude of approximately 89,000 feet. The results of limited photogrammetric instrument tests which were conducted using this photography are given along with general observations on photographic quality and the amount of detail obtainable. Illustrated.

• Book Reviews

Proceedings of the Third International Congress on High-Speed Photography

Edited by R. B. Collins. Academic Press, 111 Fifth Ave., New York 3, N.Y., 1957. 417 pp., illustrated, $13.00.

One has but to glance through current literature covering the subject of photographic instrumentation to become aware of the phenomenal developments occurring in this field, and to books such as Collins' *High-Speed Photography* we owe much for the rapid and timely dissemination of accurate information in a permanent and ready-reference form. The text covers the proceedings and discussions of the Congress held in London, England, in September 1956, under the sponsorship of the Department of Scientific and Industrial Research. All papers submitted for presentation at the Congress were screened by an editorial panel, which accepted only reports about new work, and rejected material that had been published elsewhere. As a result the papers published in these proceedings are of a high standard, describing techniques and applications not otherwise disclosed in the literature.

The following subject groups are covered: Flash Light Sources; Rotating Mirror Cameras; Mechanical Optical Drum Cameras; Inertialess Shutters; Biology and Medicine; Machine Analysis; Ballistics and Explosives; Hydrodynamics; Aerodynamics; Schlieren, Interferometric and Stereoscopic Techniques; Instrument Aids; Image-Splitting and Image-Sampling Techniques; Photographic Materials; and X-Rays and Film Evaluation. Some 60 papers included under these headings cover practically all that is new in the way of techniques, materials, and processes in the field of high-speed photography.

P. Naslin and J. S. Courtney-Pratt present excellent reviews at the beginning and end of the *Proceedings*. Naslin writes about the fundamental principles of the various systems used in high-speed photography and Courtney-Pratt discusses the papers read at the Congress.

High-Speed Photography is illustrated with some 243 excellent cuts and is a timely and valuable addition to the literature on photographic instrumentation.—*F. S.*

Bibliography on High-Speed Photography

Compiled by Elsie L. Garvin. Eastman Kodak Co., Rochester, N.Y., 1957. 35 pp.

The material published in this bibliography covering the period up to 1954 was originally compiled by Elsie L. Garvin, Librarian, Research Library, Eastman Kodak Co., and classified by John H. Wadell, Chairman of the High-Speed Photography Committee of the Society of Motion Picture and Television Engineers. This material was published in two installments in the *Journal of the SMPTE*, Vol. 56, pp. 93–111, Jan. 1951, and Vol. 61, pp. 749–757, Dec. 1953.

In the present publication, however, references have been added to cover the literature through December 1955, and they are classified, as in the earlier compilations, under the following headings: General; Cameras; Lighting; Oscillograph Photography; Schlieren Photography; Technical and Techniques; and X-Ray.—*F. S.*

Photojournalism—Pictures for Magazines and Newspapers

Arthur Rothstein. American Photographic Book Publishing Co., Inc. (Amphoto), 33 W. 60 St., New York 23, N.Y., 1956. 197 pp., $7\frac{1}{2} \times 10\frac{1}{4}$ inches, illustrated, $5.95.

This book surveys photojournalism as it is practised on magazines and newspapers. Mr. Rothstein outlines the working procedure of the news photographer, the function and responsibility of the picture editor and the art director; he explains in detail the creation of a feature picture, the construction of a photo sequence, and the principles of photographic narration; he discusses the equipment, laboratory layout and practices for this type of work; and he deals with the legal restrictions on photography, including releases and copyright. The author, who is Technical Director of *Look*, discusses the editorial procedure followed at that magazine in combining words and photographs to depict a situation or a subject.

Photojournalism is recommended to the photographic engineer who is confronted with the problem of illustrating technical projects and to those who desire to enhance the presentation of their reports.—*A. R. M.*

Photographic Abstracts—Second Decennial Index 1931–1940

The Scientific and Technical Group of the Royal Photographic Society of Great Britain, London, England, 1956. 209 pp., $6\frac{1}{4} \times 9\frac{3}{4}$ inches, £2 ($5.60).

Photographic Abstracts, a quarterly abstract journal, has been published by the Royal Photographic Society of Great Britain since 1921. It is one of the most comprehensive reference sources of the photographic literature and an indispensable part of any up-to-date photographic library.

The first ten-year index of these abstracts was published in 1932 and covered the years 1921 to 1930. The second index, published earlier this year, covers the years 1931 to 1940, and a third one is now in preparation.

The second and latest index consists of three main parts:

1. The Author Index
2. The Patent Index
3. The Subject Index

The Author and Subject Indexes are arranged alphabetically and the use of prominent headings in boldface capital letters makes it simple to locate any desired item in the Subject Index. The Patent Index, however, is arranged by patent numbers rather than by subject matter and it is necessary to refer to the Subject Index for information on patent content.

The Index is well printed and the volume bound attractively and durably. It is a valuable reference for photographic scientists and engineers.—*P. K.*

• Positions Available and Positions Wanted

Positions Available

The U.S. Army Signal Equipment Support Agency, Fort Monmouth, N.J., is seeking personnel for the following positions:

Position Title	Federal Grade	Starting Salary	Requirements
Engineer (Photographic)	GS-11	$6390 per annum	Engineering Degree plus $2\frac{1}{2}$ years general engineering experience, including 1 year specialized experience in the photographic field.
Engineer (Photographic)	GS-12	$7570 per annum	Engineering Degree plus $3\frac{1}{2}$ years general engineering experience, including 1 year specialized experience in the photographic field.
Engineer (Photographic)	GS-13	$8990 per annum	Engineering Degree plus 4 years general engineering and administrative experience, including 1 year specialized experience in the photographic field.

Applicants should contact the Civilian Personnel Office, Employee Utilization Division, Building 787, Fort Monmouth, N.J., as soon as possible. All positions will be located in the vicinity of Fort Monmouth, with a minor amount of travel involved.

Members of the Society are invited to make use of this department when seeking personnel or positions. The space is available without charge. Address inquiries to the Editorial Vice President, Peter Krause, 69 Bourndale Road South, Manhasset, N.Y.

The Society of Photographic Scientists and Engineers

Box 1609 • Main Post Office • Washington, D.C.

OFFICERS

President	GEORGE T. EATON, Bldg. 59, Kodak Park, Rochester 4, New York
Executive Vice President	STEVEN LEVINOS, Ansco, Binghamton, New York
Engineering Vice President	JOHN A. MAURER, 116–118 West 29th Street, New York 1, New York
Editorial Vice President	PETER KRAUSE, 69 Bourndale Road South, Manhasset, New York
Financial Vice President	HERBERT MEYER, 325 Sequoia Drive, Pasadena 2, California
Secretary-Treasurer	NORTON GOODWIN, 826 Connecticut Avenue NW, Washington 6, D.C.
Managing Secretary	EDWARD S. COBB, Box 1609, Main Post Office, Washington, D.C.

CHAPTERS *and* CHAPTER OFFICERS

Binghamton, New York	*President*	KEITH FAMULENER, 605 Main Street, Owego, New York
	Secretary	L. A. MICCO, 125 Leroy Street, Binghamton, New York
Boston, Massachusetts	*President*	LOUIS ROSENBLUM, Photon, Inc., 58 Charles Street, Cambridge 41, Mass.
	Secretary	E. FRANCIS MACNEILL, 253 Greendale Avenue, Needham 94, Mass.
Cleveland, Ohio	*President*	W. H. BOWERMAN, Box 154, Solon, Ohio
	Secretary	CLINTON K. HAMLINK, 2230 South Overlook Road, Cleveland 6, Ohio
Ithaca, New York	*President*	ARTHUR C. STALLMAN, 218 Waite Avenue, Ithaca, New York
	Secretary	DAVID O. FLETCHER, 1314 East State Street, Ithaca, New York
Monmouth, New Jersey	*President*	THEODORE CATELLI, 37 Brook Avenue, Little Silver, New Jersey
	Secretary	JOSEPH MANGIARACINA, 30 Brook Avenue, Little Silver, New Jersey
New York, New York	*President*	HENRY M. LESTER, 270 West End Avenue, New York 23, New York
	Secretary	RALPH R. BAUM, 319 East 44th Street, New York 17, New York
Rochester, New York	*President*	WILLIAM S. SHOEMAKER, Rochester Institute of Technology, 65 South Plymouth Avenue, Rochester, New York
	Secretary	ROBERT H. MAHER, Eastman Kodak Company, 343 State Street, Rochester 4, New York
Southern California	*President*	ROBERT O. MEASE, 26707 Eastvale Road, Rolling Hills, California
	Secretary	BERNARD A. AUGUSTINE, 235 Annandale Road, Pasadena 1, California
Southern Lake Michigan	*President*	N. W. RODELIUS, 2749 Reese Avenue, Evanston, Illinois
	Secretary	ROBERT J. MAZOR, 1438 West 123rd Street, Chicago 43, Illinois
Washington, D.C.	*President*	HOWLAND PIKE, RFD 2, Silver Spring, Maryland
	Secretary	DWIN R. CRAIG, 815 Fisher Street, Falls Church, Virginia
Mid-Gulf Area	*Organizing Committee*	ROBERT E. LEWIS, CML, University of Chicago, Eglin Air Base, Florida

Sustaining Members / Society of Photographic Scientists and Engineers

Abrams Aerial Survey Corporation

Ansco

Argus Camera

Charles Austin, Incorporated

Bar-Ray Products, Incorporated

Bausch & Lomb Optical Company

Bell & Howell Company

Charles Beseler Company

Cameraflex, Incorporated

Chemco Photoproducts Company, Incorporated

Chicago Aerial Industries, Incorporated

De Jur Amsco Corporation

E. I. du Pont de Nemours & Company

Eastman Kodak Company

Ednalite Optical Company, Incorporated

Elgeet Optical Company, Incorporated

Enteco Industries, Incorporated

Fairchild Camera & Instrument Corporation

Farrand Optical Company, Incorporated

Federal Manufacturing & Engineering Corporation

Oscar Fisher Company, Incorporated

The F-R Corporation

General Electric Company

Gordon Enterprises

Graflex, Incorporated

Grant Photo Products

W. & L. E. Gurley Company

The Haloid Company

Hardale Associates

Harris-Seybold Company

Horizons, Incorporated

Hycon Manufacturing Company

Houston Fearless Corporation

Charles A. Hulcher Company

Philip A. Hunt Company

Bill Jack Scientific Instrument Company

Kalart, Incorporated

Kollmorgen Optical Corporation

J. A. Maurer, Incorporated

The Morse Instrument Company

Nems-Clarke, Incorporated

Pako Corporation

Photogrammetry, Incorporated

Polaroid Corporation

Remington Rand, Incorporated

Simmon Brothers, Incorporated

Sun Ray Photo Products, Incorporated

Technicolor New York Corporation

Wollensak Optical Company

Zoomar, Incorporated